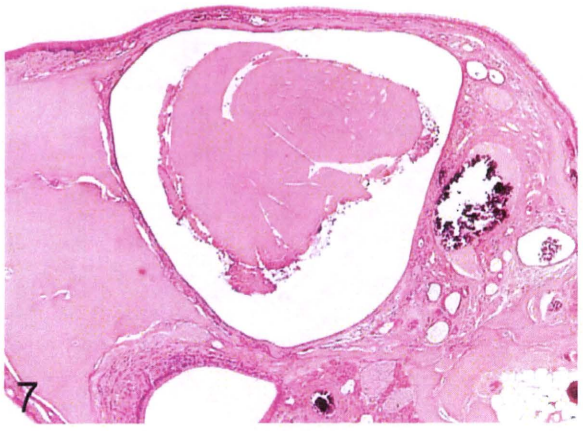

FIGURE 7.—Rat. Cystic dilatation and degeneration, vomeronasal organ.

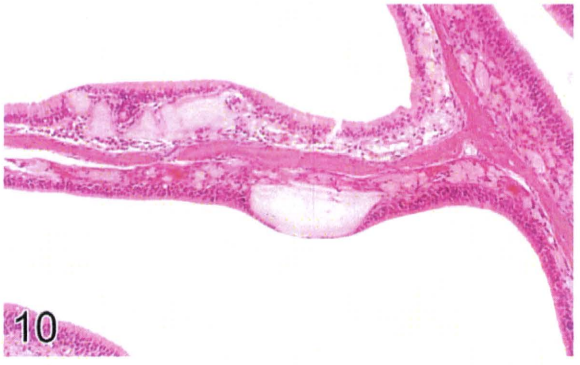

FIGURE 10.—Rat. Corpora amylacea in ethmoturbinates.

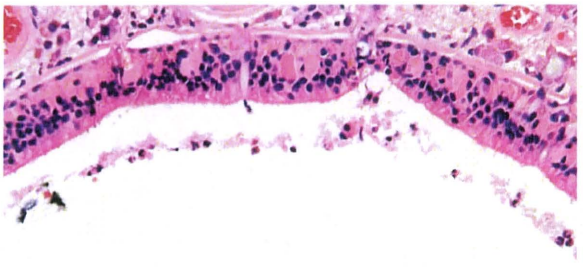

FIGURE 8.—Rat. Eosinophilic globules in olfactory epithelium.

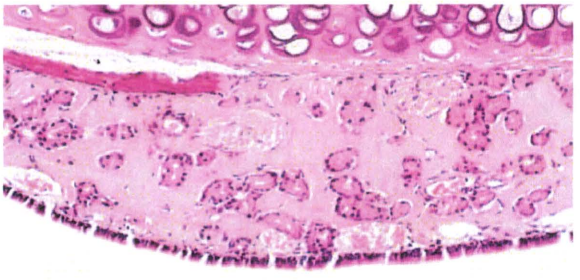

FIGURE 11.—Mouse. Amyloid in submucosa of nasal septum.

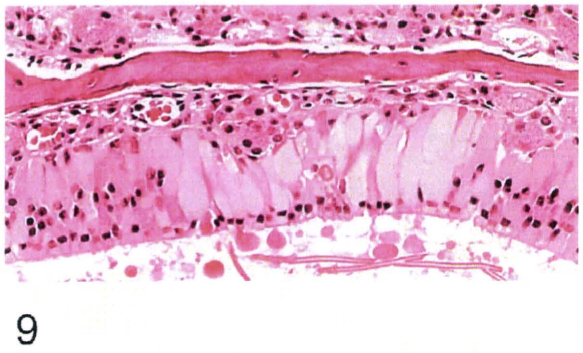

FIGURE 9.—Mouse. Olfactory epithelial degeneration and eosinophilic globules in olfactory epithelium.

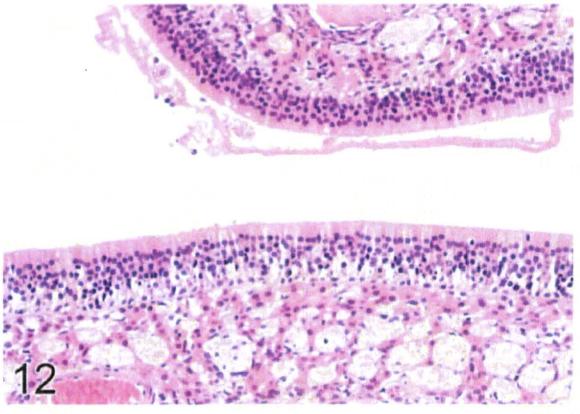

FIGURE 12.—Rat. Early necrosis, olfactory epithelium

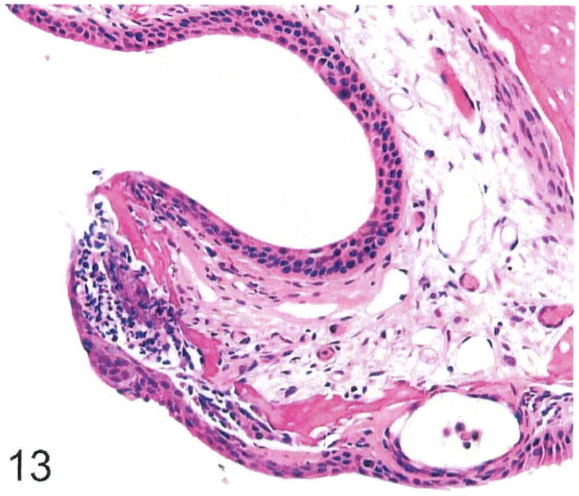

FIGURE 13.—Mouse. Necrosis, inflammation, and squamous metaplasia, turbinate.

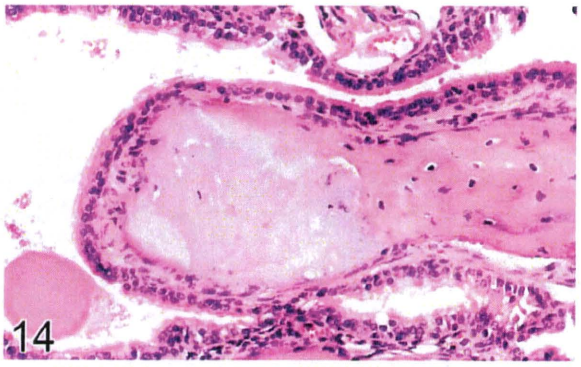

FIGURE 14.—Mouse. Necrosis of nasal turbinate.

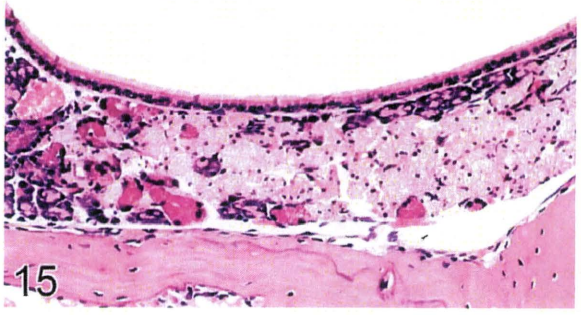

FIGURE 15.—Mouse. Necrosis, Steno's glands.

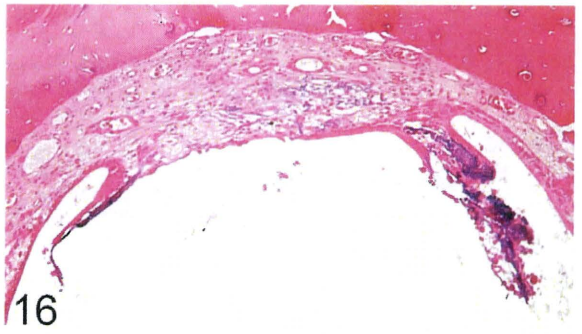

FIGURE 16.—Rat. Ulceration of olfactory epithelium.

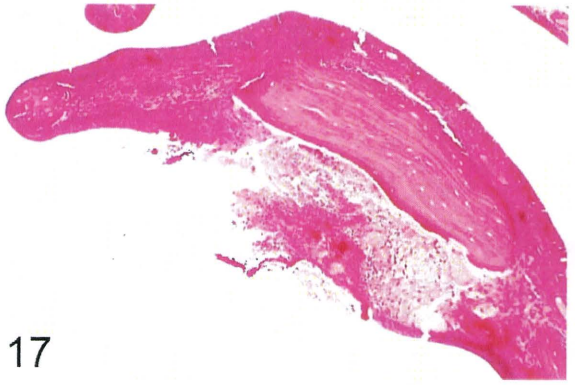

FIGURE 17.—Rat. Ulceration and suppurative inflammation, nasal turbinate.

FIGURE 18.—Rat. Synechia and osteofibrosis in ethmoturbinates.

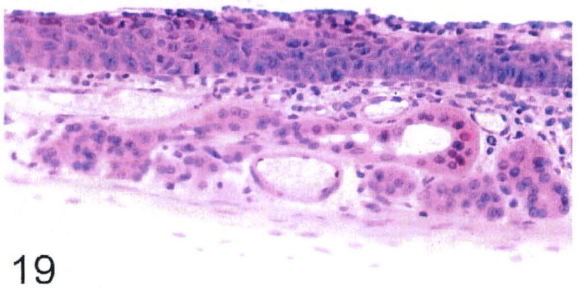

FIGURE 19.—Rat. Regeneration of olfactory epithelium.

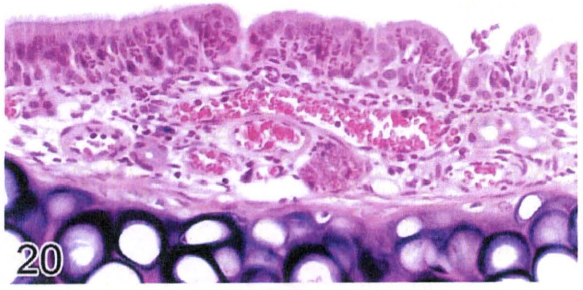

FIGURE 20.—Mouse. Suppurative inflammation and hyperplasia.

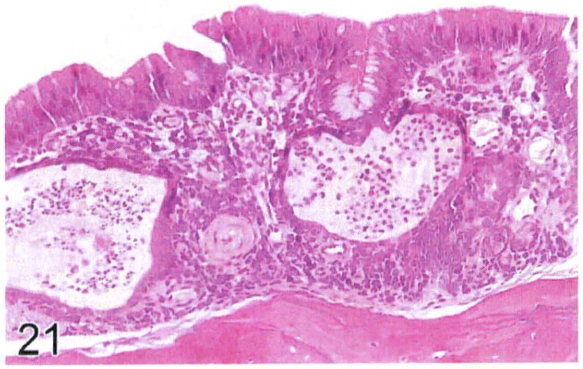

FIGURE 21.—Rat. Chronic inflammation, olfactory epithelium.

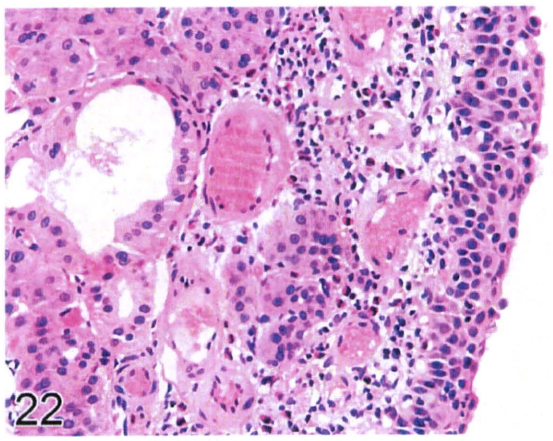

FIGURE 22.—Mouse. Chronic active inflammation, nasal septum.

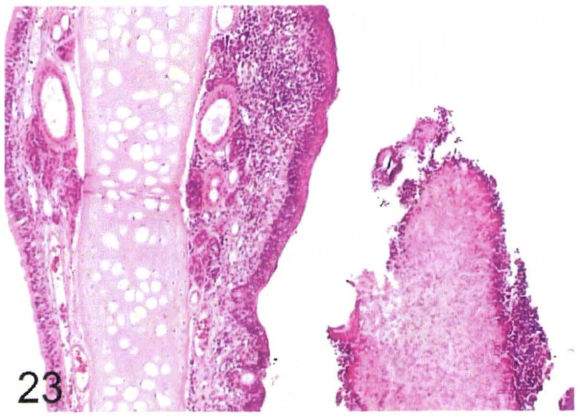

FIGURE 23.—Rat. Nasal cavity, granulomatous inflammation.

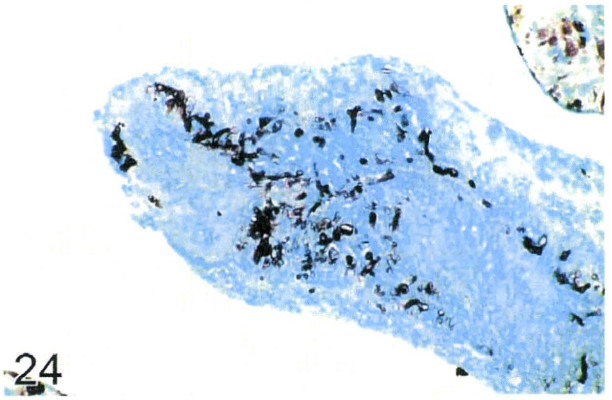

FIGURE 24.—Rat. Fungal granuloma in nasal cavity, silver stain.

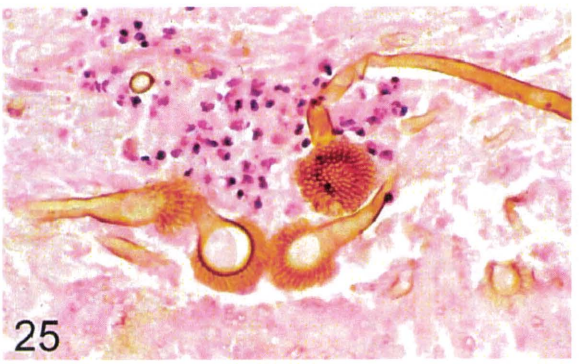

FIGURE 25.—Rat. Fungal colonies in nasal cavity, fungal stain.

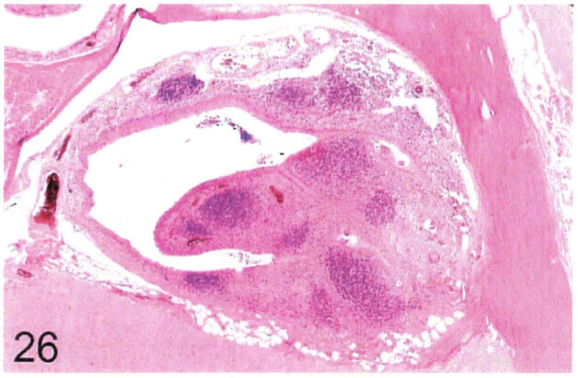

FIGURE 26.—Rat. Granulomatous inflammation, nasolacrimal duct.

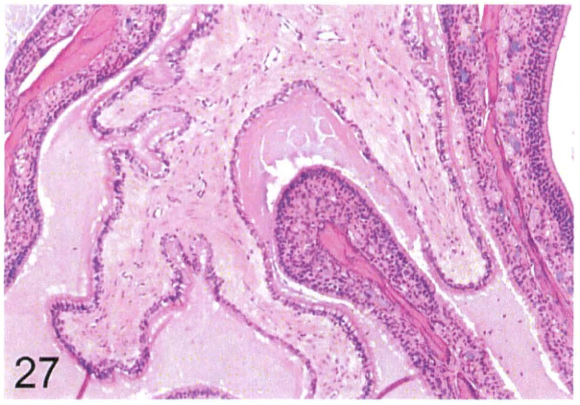

FIGURE 27.—Mouse. Inflammatory polyp extending around ethmoturbinates.

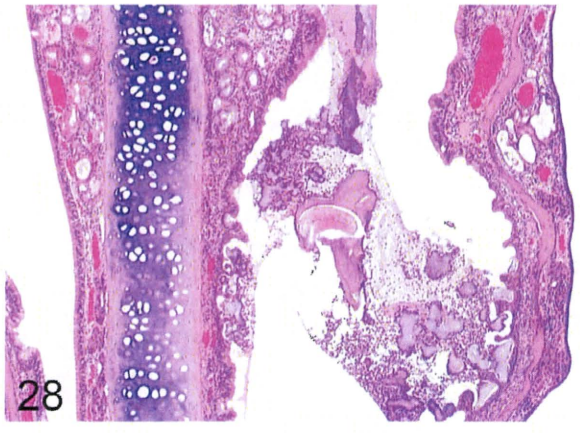

FIGURE 28.—Rat. Foreign body in nasal lumen with inflammatory exudate.

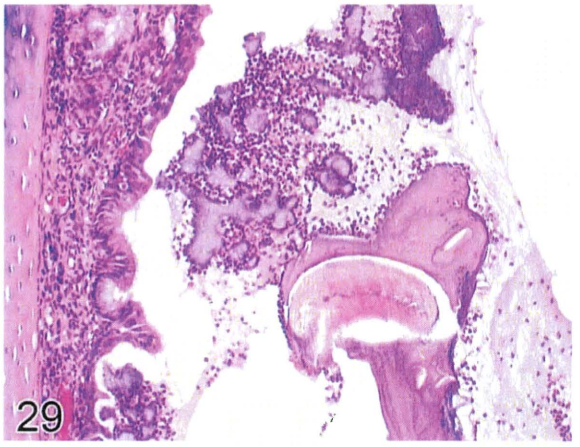

FIGURE 29.—Rat. Higher power of Figure 28, foreign body in nasal lumen.

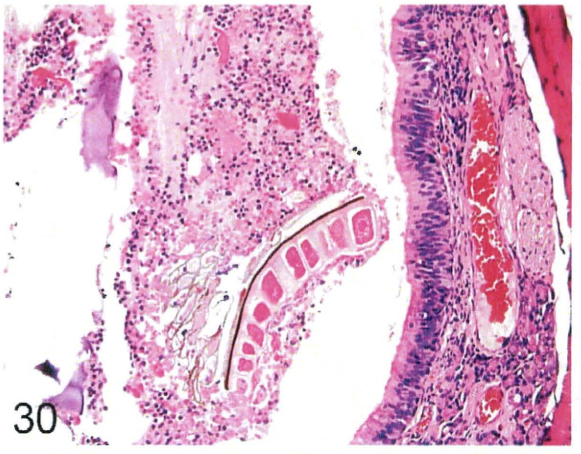

FIGURE 30.—Rat. Plant material in nasal lumen with inflammatory exudate.

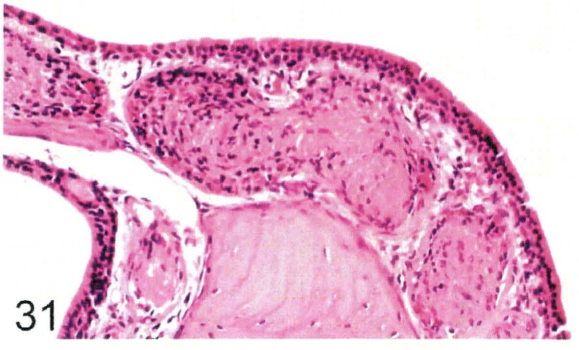

FIGURE 31.—Rat. Thrombi in submucosal vessels of nasal cavity.

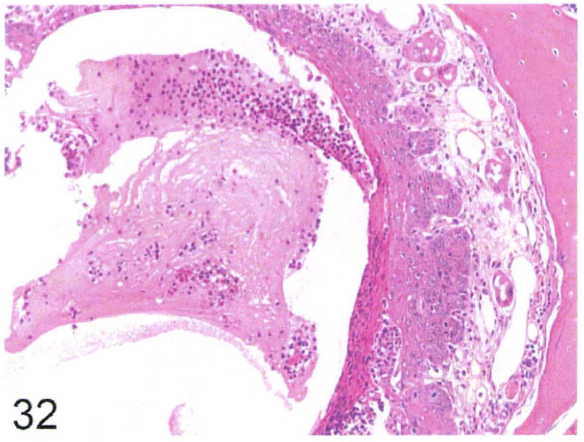

FIGURE 32.—Mouse. Nasal cavity, squamous cell metaplasia.

FIGURE 35.—Rat. Nasal cavity, transitional epithelium, hyperplasia.

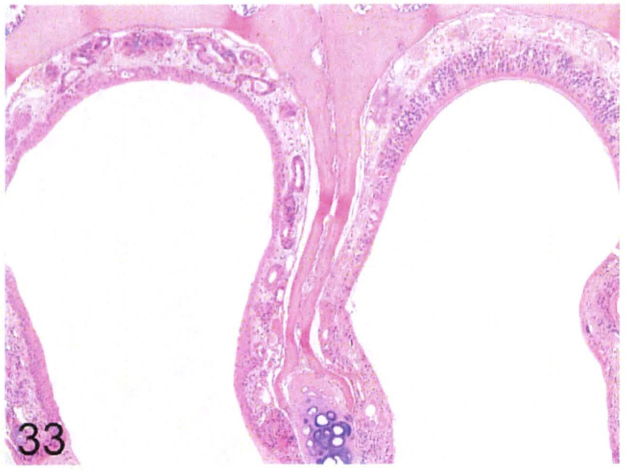

FIGURE 33.—Mouse. Nasal cavity, respiratory metaplasia of olfactory epithelium.

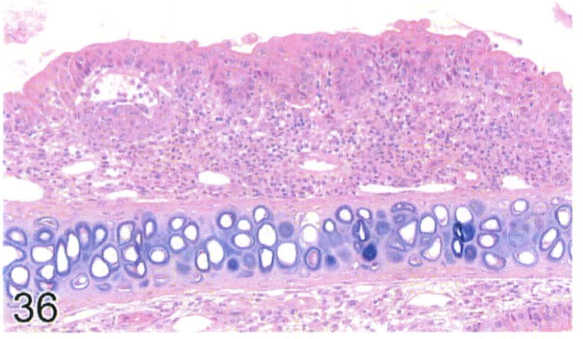

FIGURE 36.—Rat, Nasal cavity, respiratory epithelium, hyperplasia.

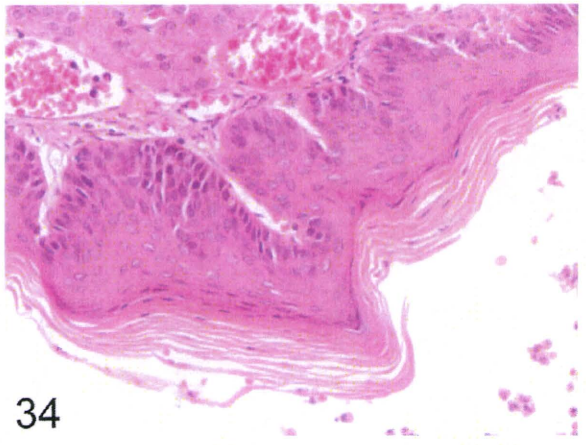

FIGURE 34.—Rat. Nasal cavity, squamous epithelium, hyperplasia.

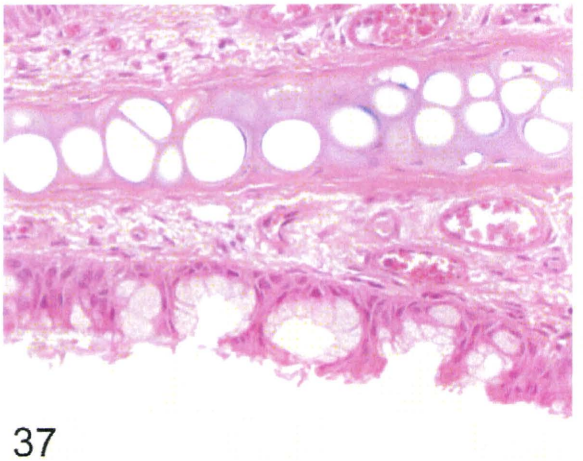

FIGURE 37.—Rat. Nasal cavity, mucous cell hyperplasia.

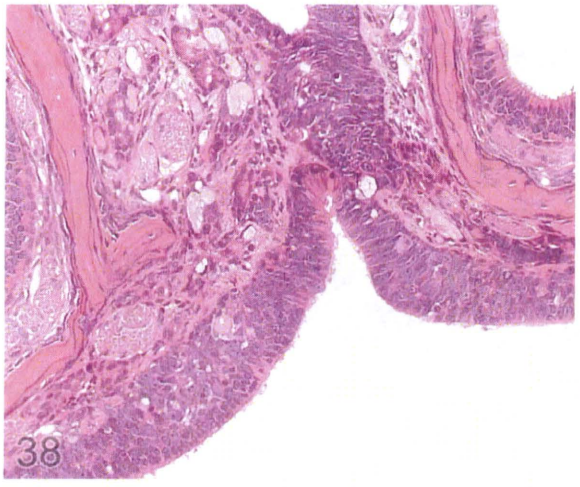

FIGURE 38.—Rat. Nasal cavity, olfactory epithelium, hyperplasia.

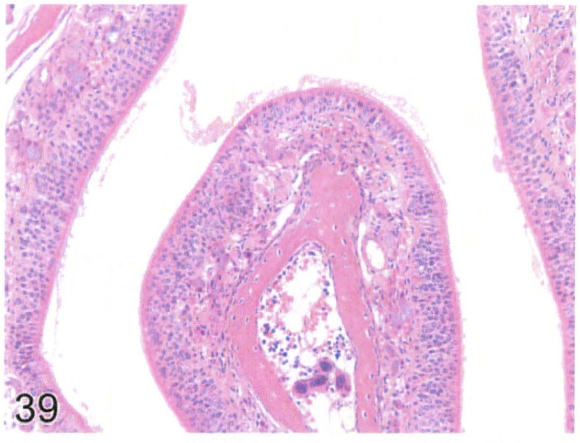

FIGURE 39.—Mouse. Nasal cavity, basal cell hyperplasia.

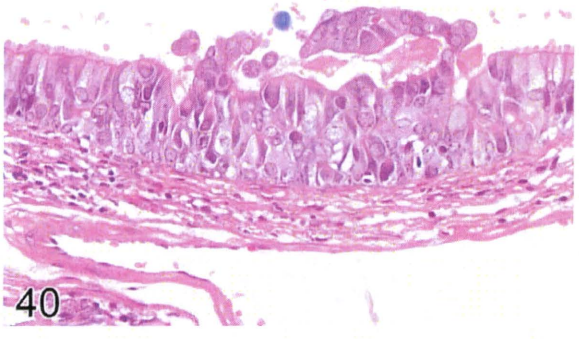

FIGURE 40.—Rat. Nasal cavity, respiratory epithelium, hyperplasia with cellular atypia.

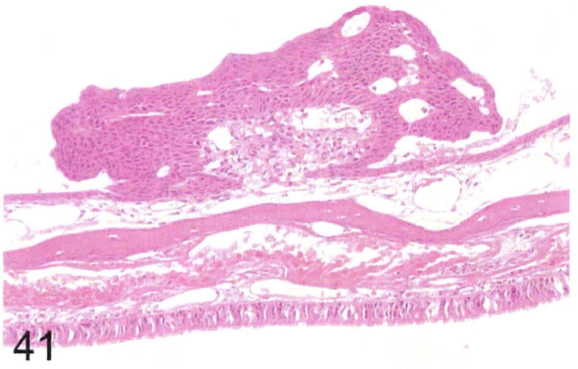

FIGURE 41.—Rat. Nasal cavity, papilloma.

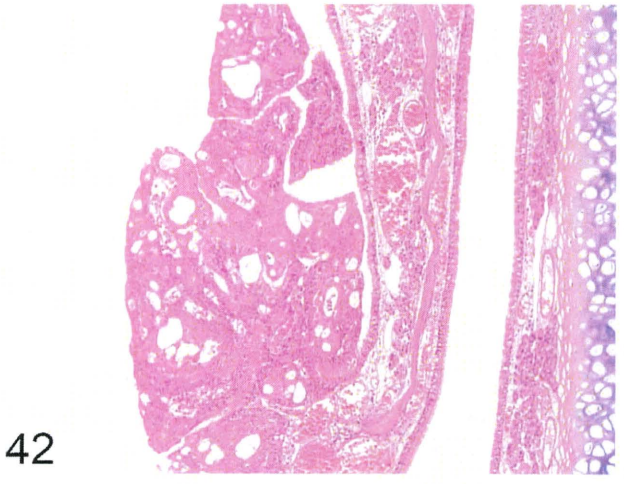

FIGURE 42.—Rat. Nasal cavity, adenoma.

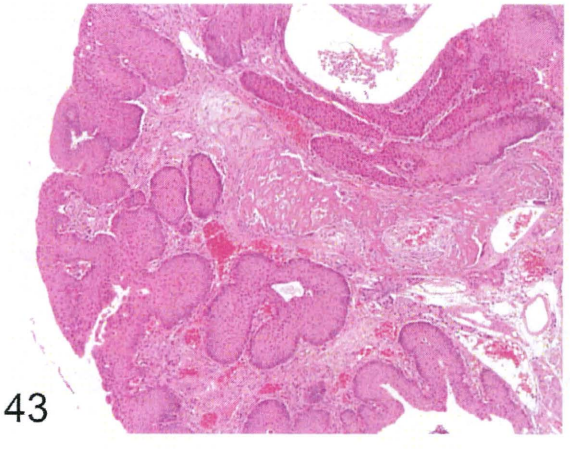

FIGURE 43.—Rat. Nasal cavity, carcinoma, squamous.

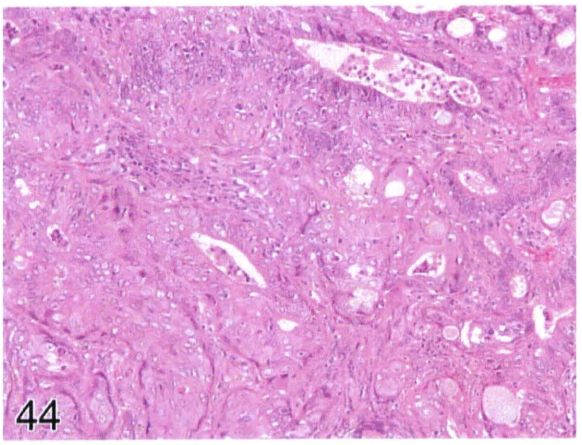

FIGURE 44.—Rat. Nasal cavity, carcinoma, adenosquamous.

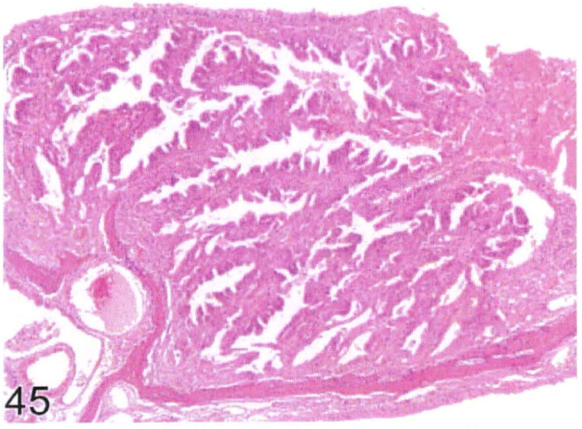

FIGURE 45.—Rat. Nasal cavity, adenocarcinoma.

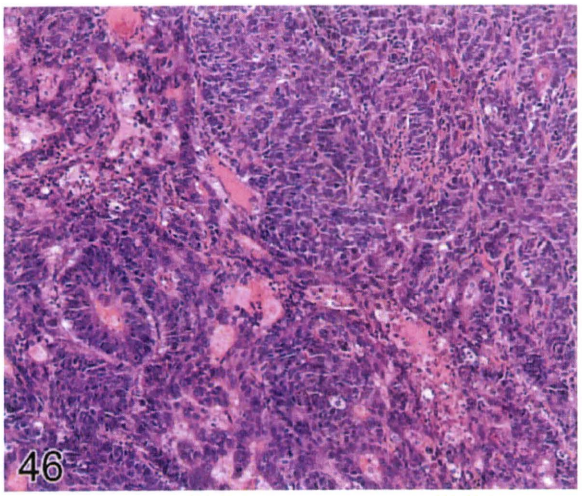

FIGURE 46.—Rat, Nasal cavity, carcinoma, neuroepithelial.

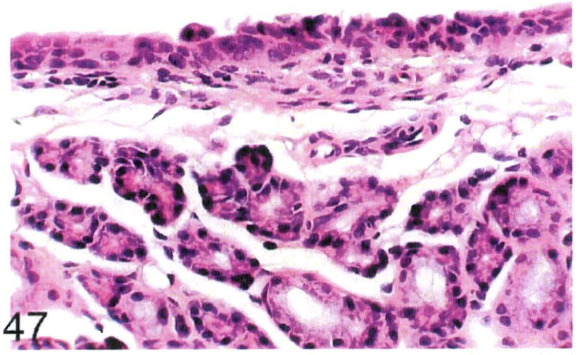

FIGURE 47.—Mouse. Epiglottis, epithelial degeneration and acute inflammation.

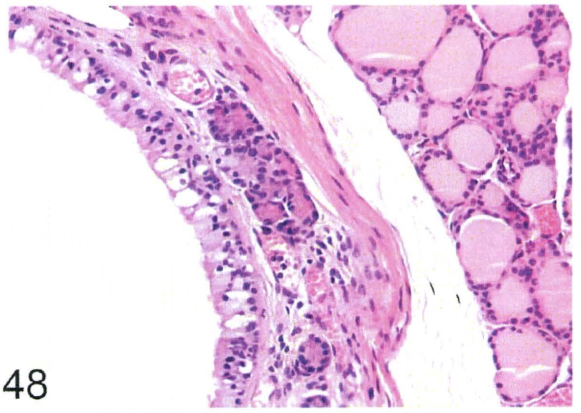

FIGURE 48.—Mouse. Tracheal epithelium, degeneration.

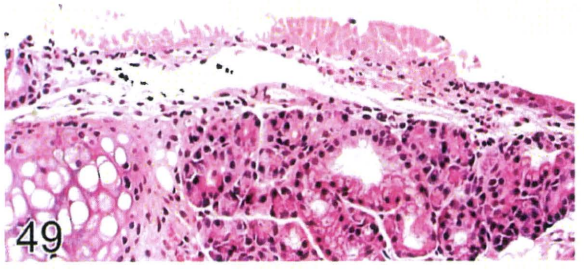

FIGURE 49.—Mouse. Epiglottis, acute epithelial necrosis.

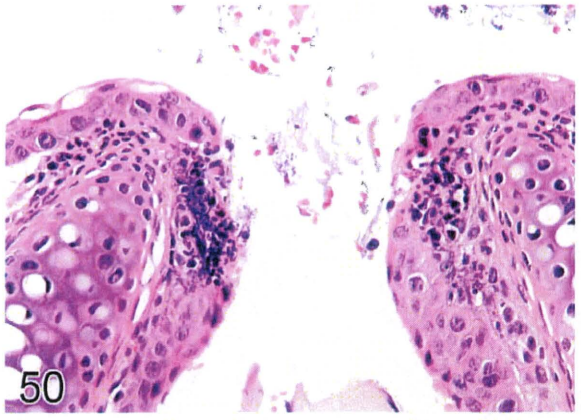

FIGURE 50.—Mouse. Larynx, necrosis and inflammation, tips of arytenoid process.

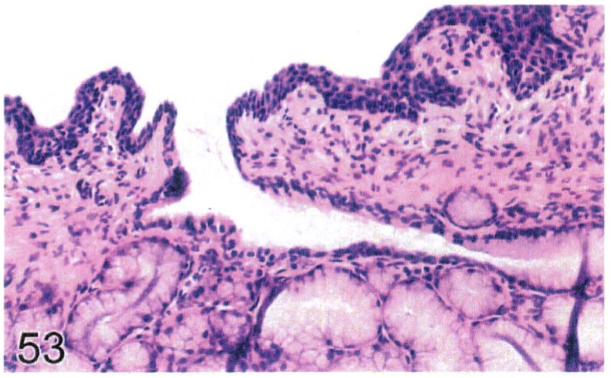

FIGURE 53.—Rat. Epiglottis, squamous metaplasia extending into submucosal gland duct.

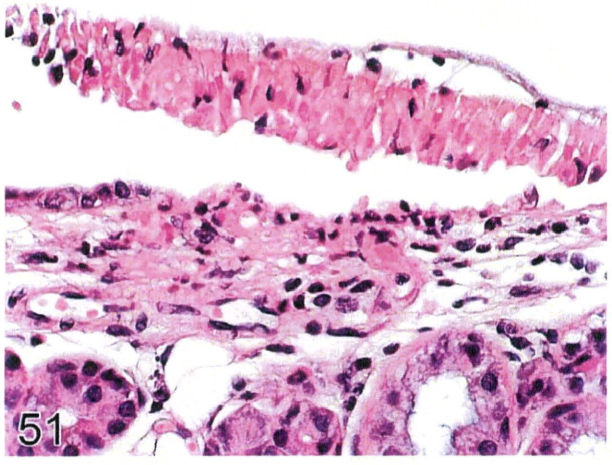

FIGURE 51.—Mouse. Epiglottis, epithelial necrosis and ulceration.

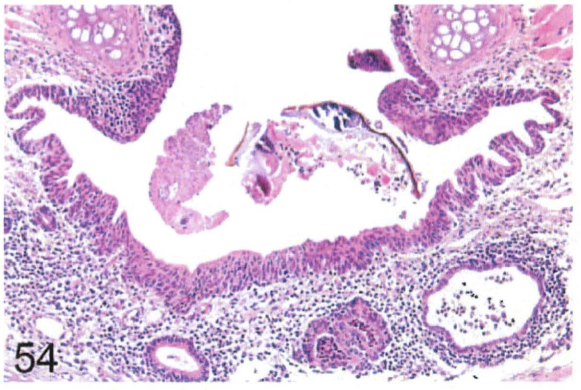

FIGURE 54.—Mouse. Larynx, chronic inflammation and foreign body, ventral pouch.

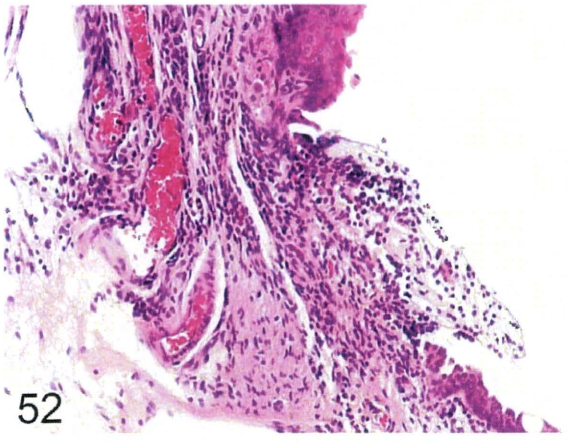

FIGURE 52.—Rat. Epiglottis, ulceration and suppurative inflammation.

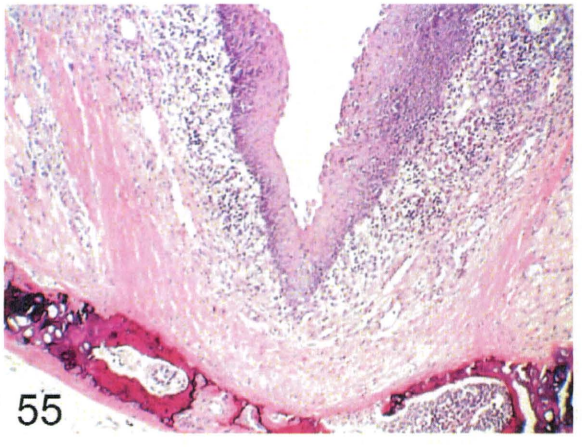

FIGURE 55.—Rat. Caudal larynx, chronic inflammation, squamous metaplasia, and hyperplasia.

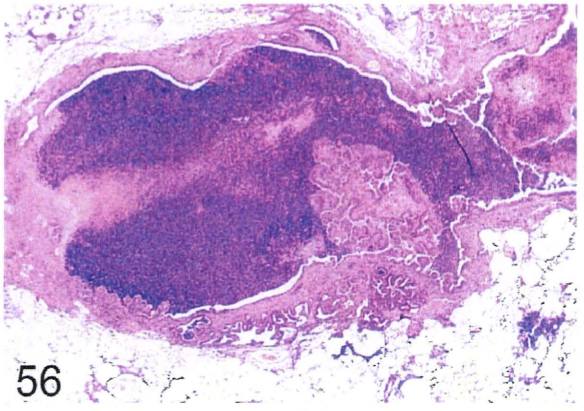

FIGURE 56.—Rat. Bronchiectasis with epithelial hyperplasia, suppurative exudate.

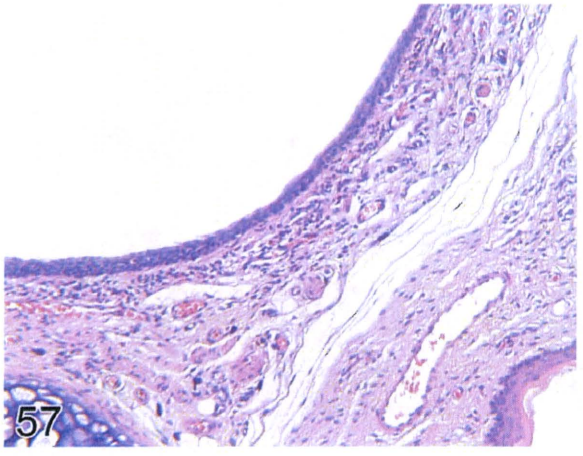

FIGURE 57.—Rat. Epiglottis, epithelial alteration.

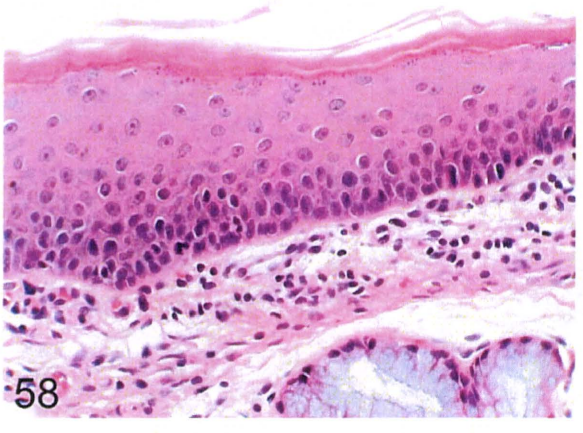

FIGURE 58.—Rat. Epiglottis, squamous metaplasia, hyperplasia, and keratinization.

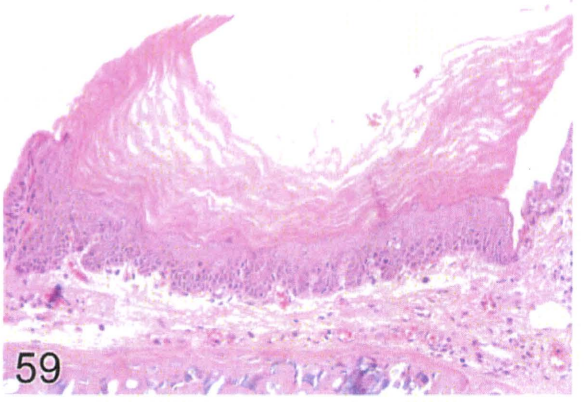

FIGURE 59.—Rat. Trachea, squamous metaplasia, epithelium.

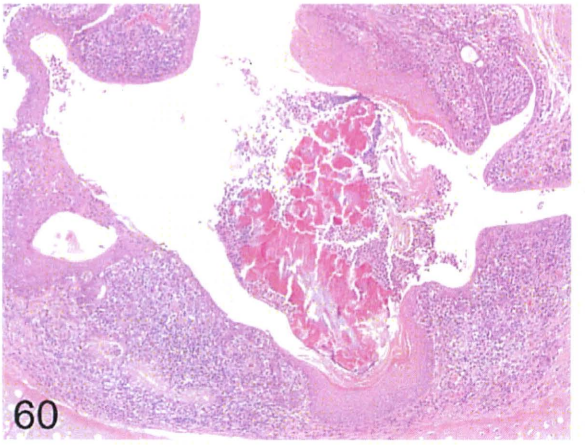

FIGURE 60.—Rat. Larynx, squamous metaplasia and hyperplasia, ventral pouch.

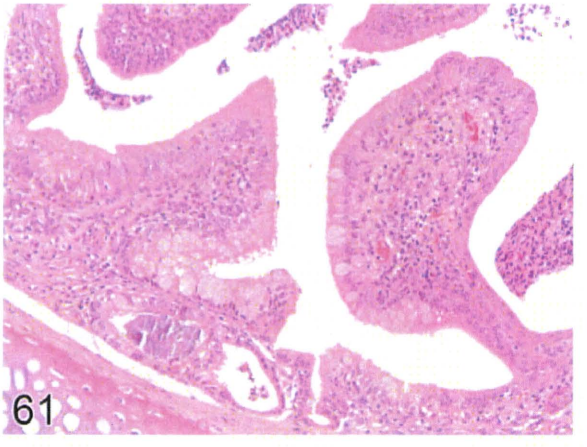

FIGURE 61.—Rat. Larynx, hyperplasia, respiratory epithelium.

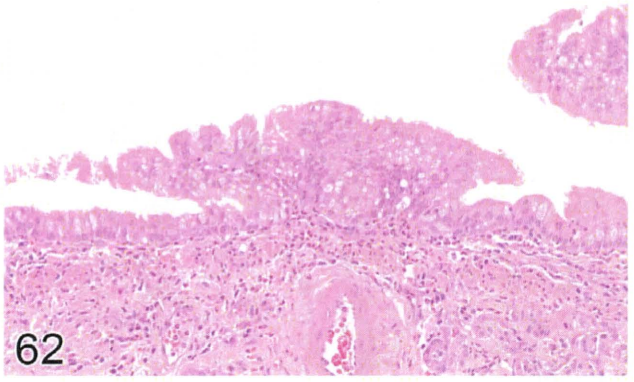

FIGURE 62.—Rat. Bronchus, hyperplasia, mucous cells.

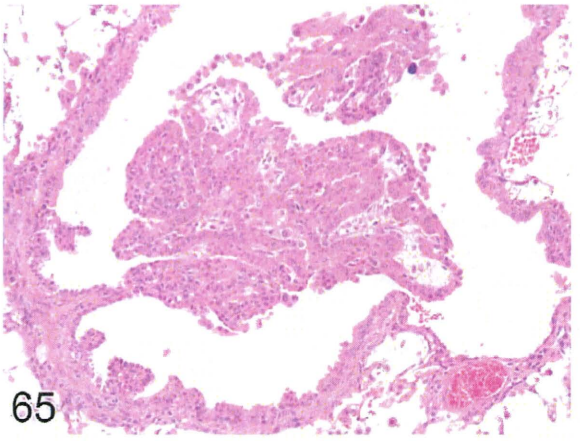

FIGURE 65.—Mouse. Bronchus, papilloma.

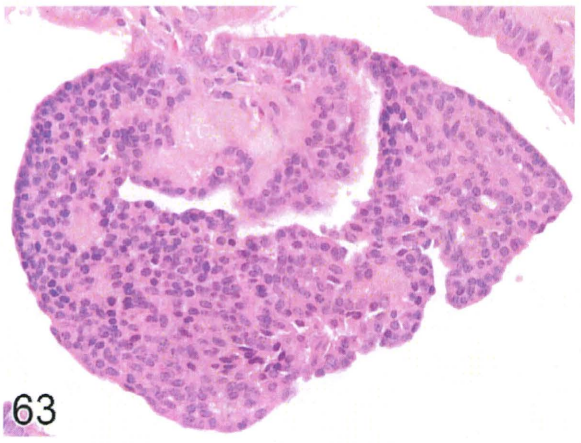

FIGURE 63.—Rat. Bronchus, hyperplasia, neuroendocrine cells.

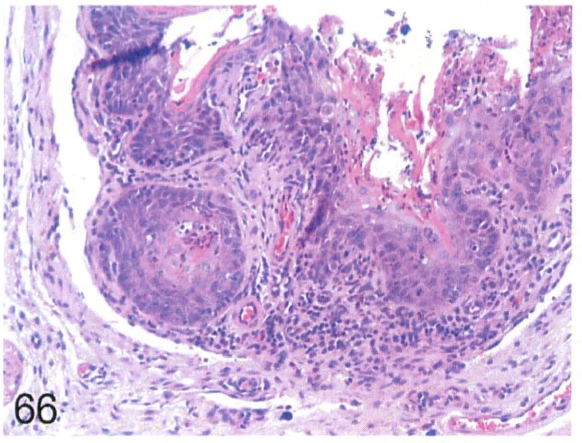

FIGURE 66.—Rat. Laryngopharynx, carcinoma, squamous cell.

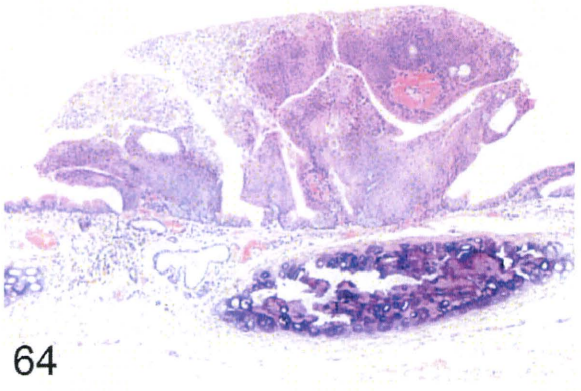

FIGURE 64.—Rat. Trachea, papilloma, squamous cell.

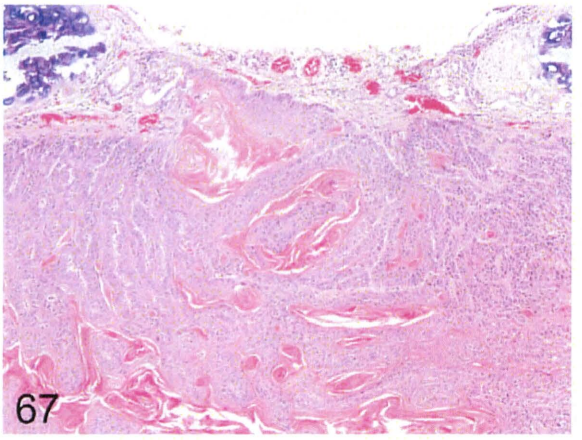

FIGURE 67.—Rat. Trachea, carcinoma, squamous cell.

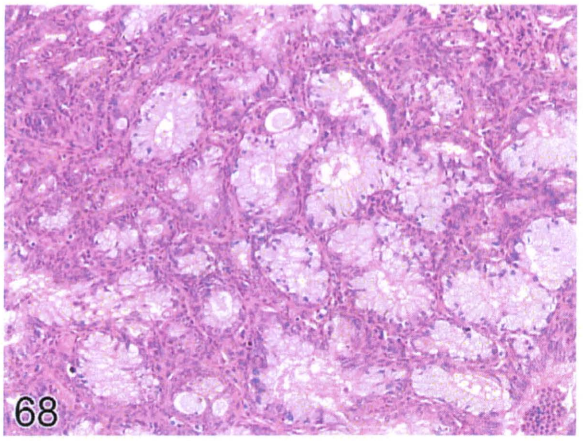

FIGURE 68.—Rat. Bronchus, adenocarcinoma.

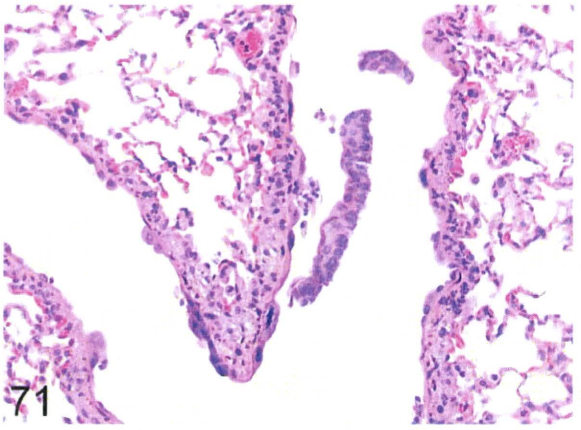

FIGURE 71.—Mouse. Bronchiole, epithelial degeneration, necrosis, regeneration.

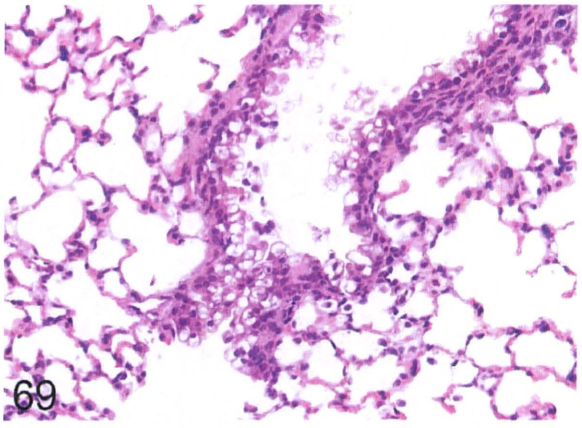

FIGURE 69.—Mouse. Bronchiole, cytoplasmic vacuolation, epithelium.

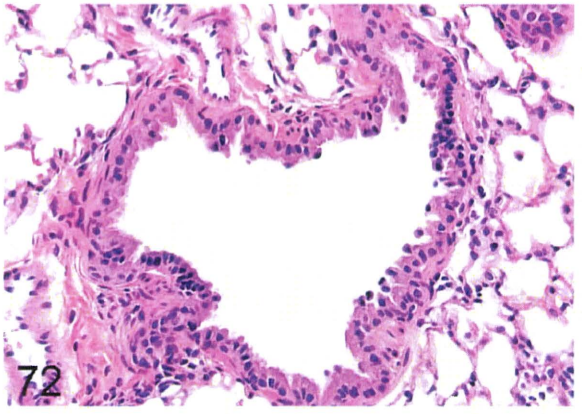

FIGURE 72.—Mouse. Bronchiole, epithelial regeneration.

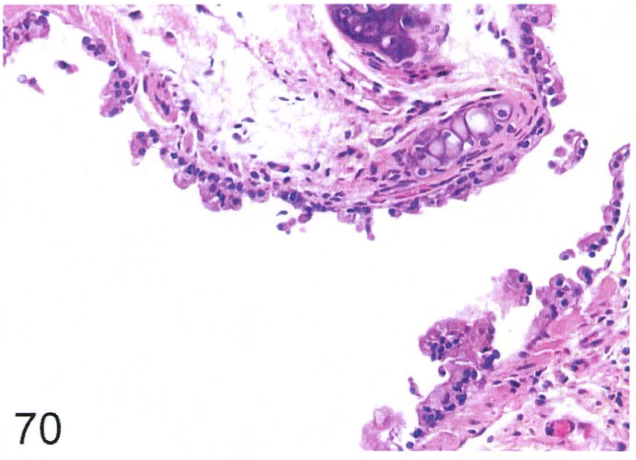

FIGURE 70.—Mouse. Bronchiole, epithelial necrosis.

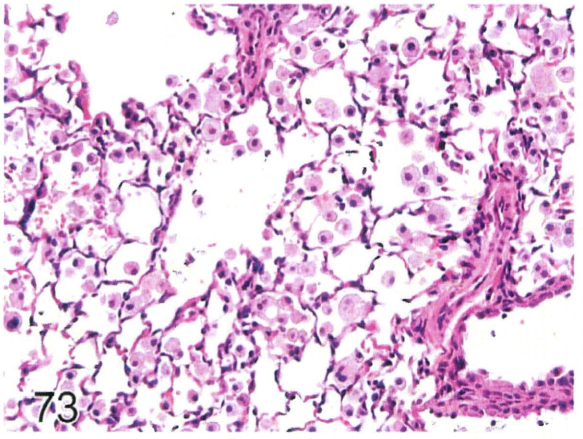

FIGURE 73.—Mouse. Lung, aggregates of alveolar macrophages (histiocytosis).

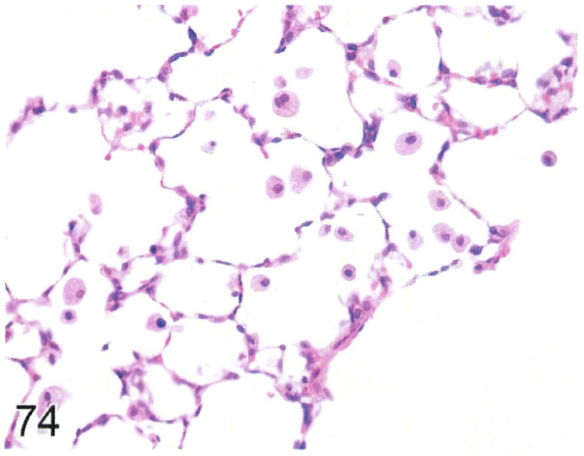

FIGURE 74.—Rat. Lung, phospholipidosis.

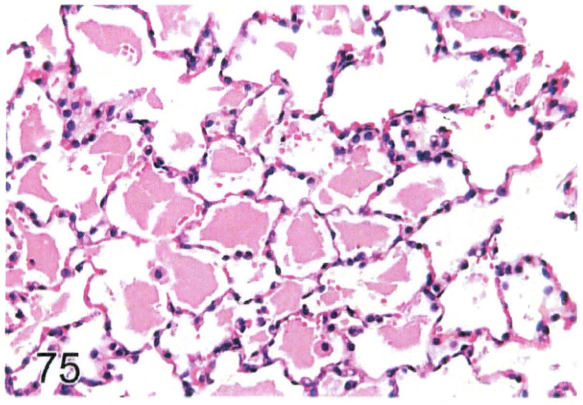

FIGURE 75.—Rat. Lung, alveolar lipoproteinosis.

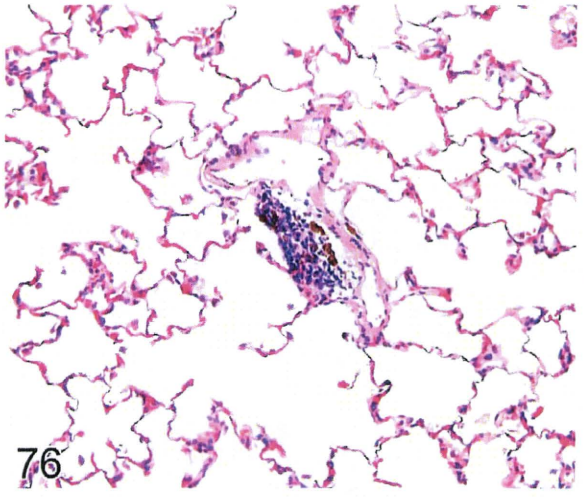

FIGURE 76.—Rat. Lung, hemosiderin pigment in perivascular macrophages.

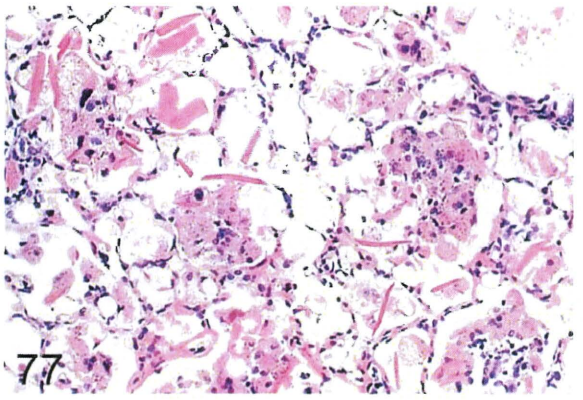

FIGURE 77.—Mouse. Lung, hemoglobin crystals in macrophages and alveoli.

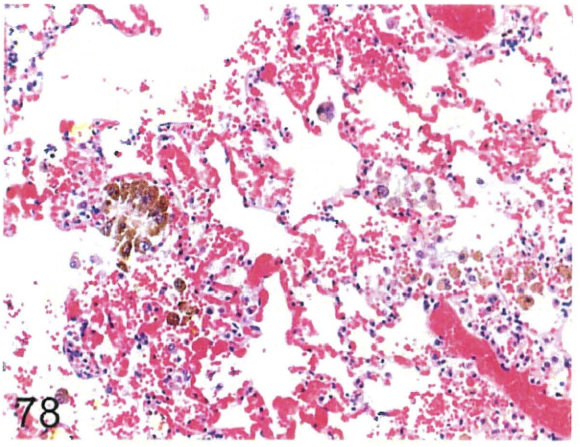

FIGURE 78.—Rat. Lung, phagocytized corn oil in alveolar macrophages.

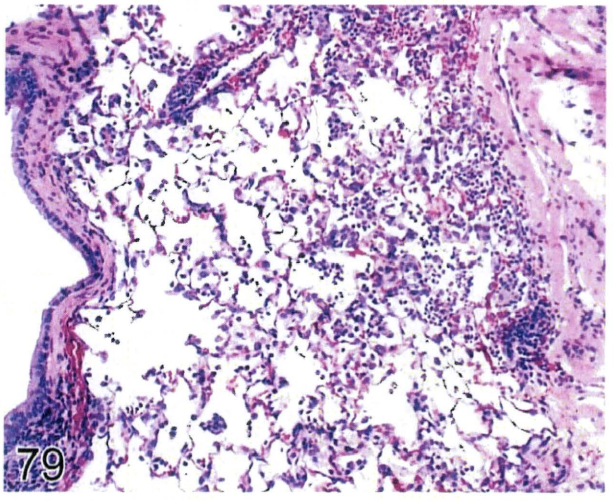

FIGURE 79.—Rat. Lung, suppurative perivascular and alveolar infiltrate.

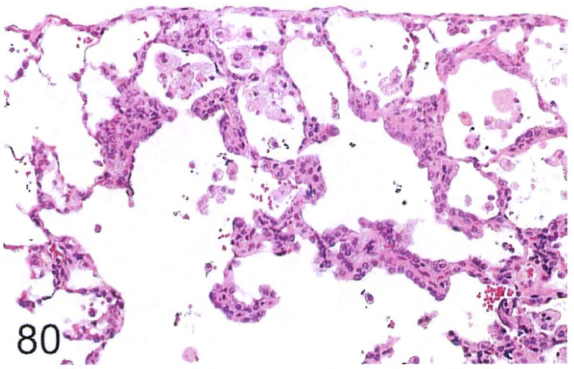

FIGURE 80.—Rat. Lung, chronic interstitial inflammation, subpleural.

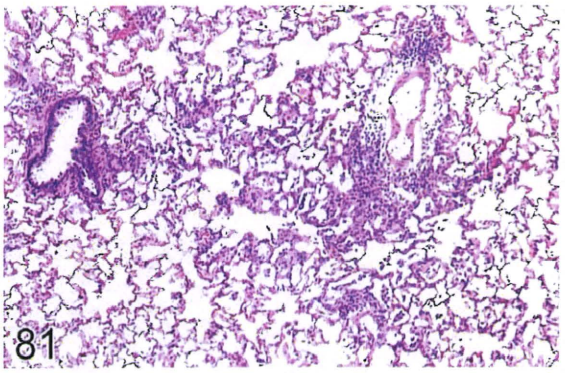

FIGURE 81.—Rat. Lung, chronic interstitial inflammation in lung parenchyma.

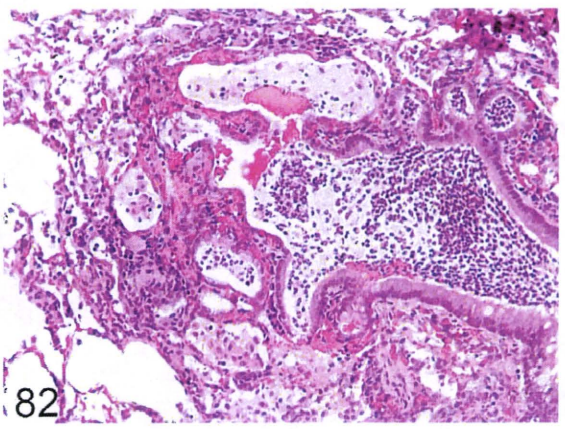

FIGURE 82.—Rat. Lung, suppurative infiltrate in bronchiole and alveoi (bronchopneumonia).

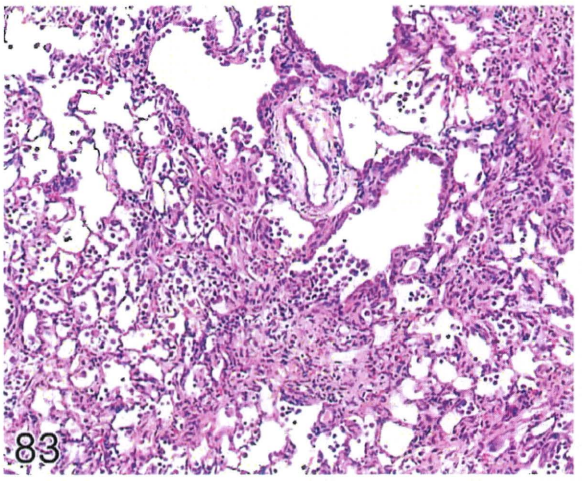

FIGURE 83.—Rat. Lung, mixed inflammatory infiltrate and early alveolar fibrosis.

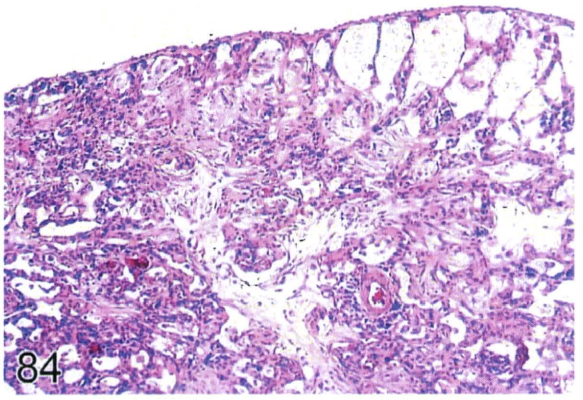

FIGURE 84.—Rat. Lung, chronic inflammation with fibrosis.

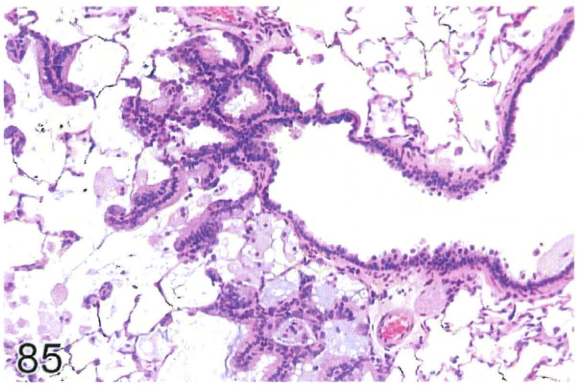

FIGURE 85.—Rat. Lung, bronchiolization of alveolar epithelium.

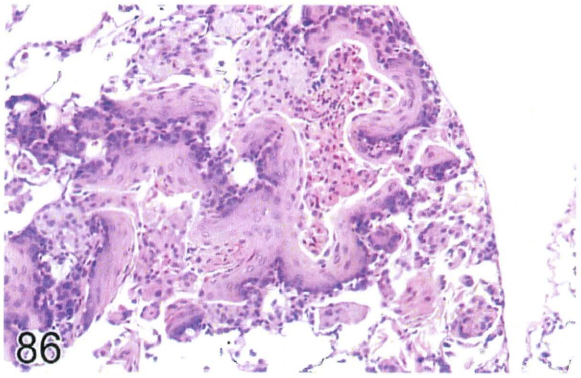

FIGURE 86.—Rat. Lung, squamous metaplasia of alveolar epithelium.

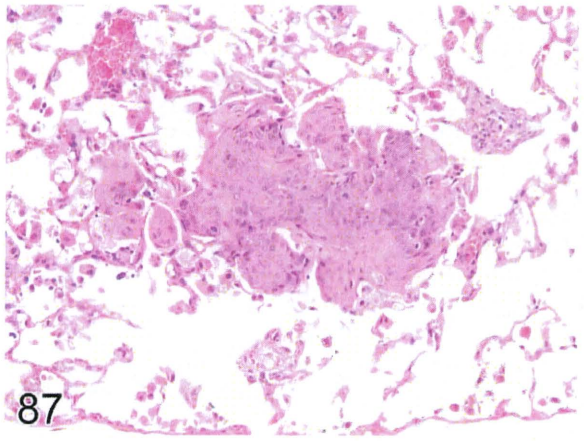

FIGURE 87.—Rat. Lung, squamous metaplasia of alveolar epithelium.

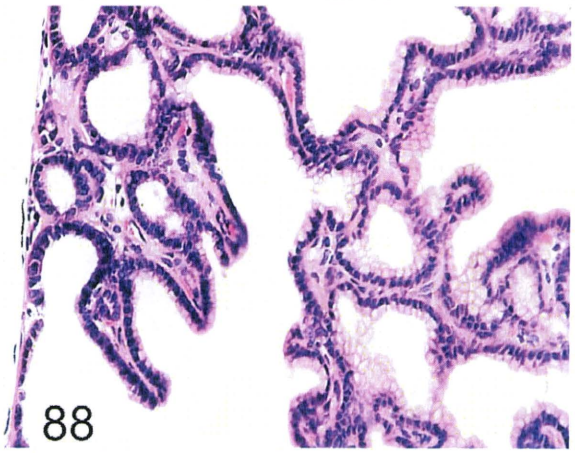

FIGURE 88.—Mouse. Lung, mucous (goblet) cell metaplasia of alveolar epithelium.

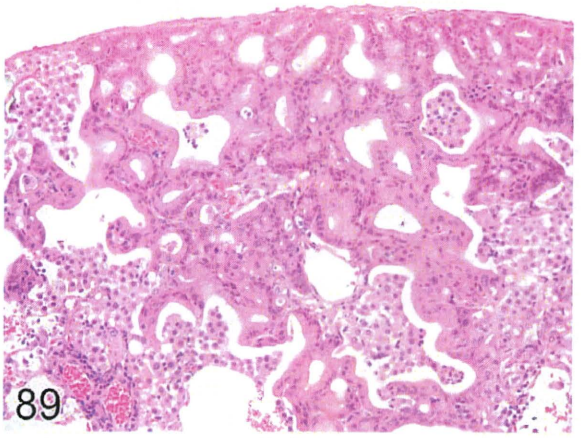

FIGURE 89.—Mouse. Lung, mucous (goblet) cell metaplasia of alveolar epithelium.

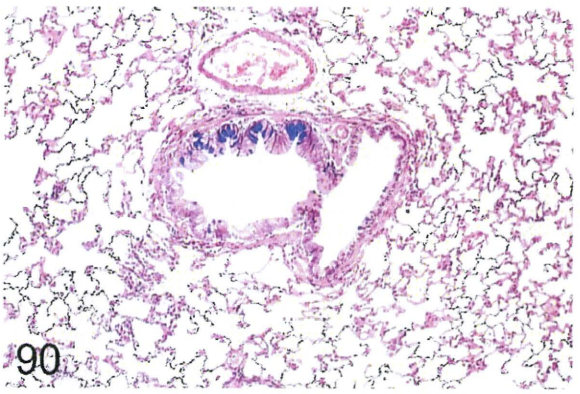

FIGURE 90.—Rat. Bronchiole, mucous metaplasia, Alcian Blue stain.

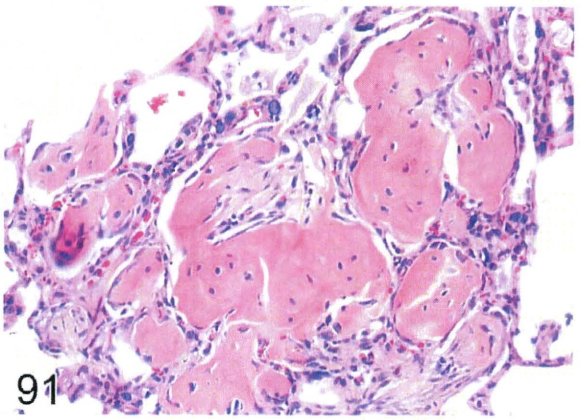

FIGURE 91.—Rat. Lung, osseous metaplasia in alveoli.

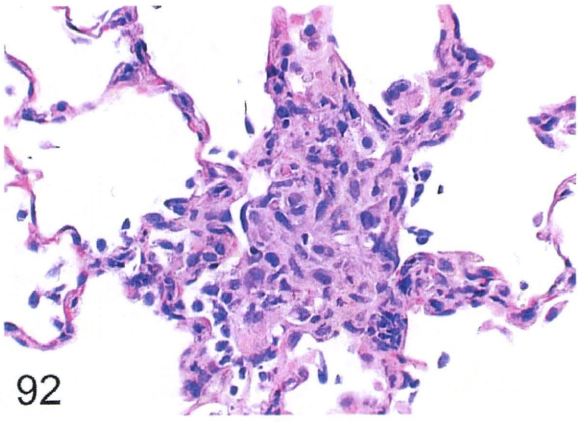

FIGURE 92.—Mouse. Lung, focal granulomatous inflammation in alveoli.

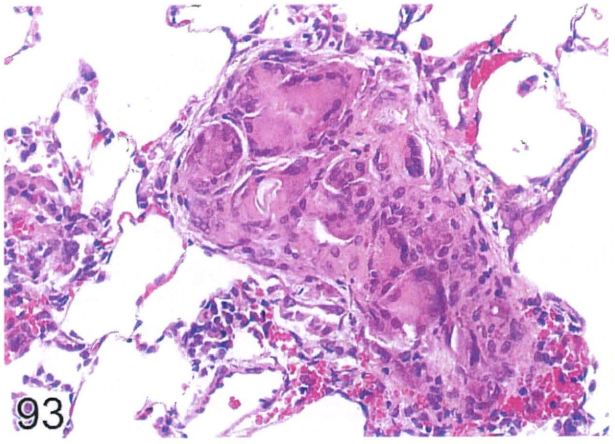

FIGURE 93.—Rat. Lung, multinucleated giant cells and foreign body.

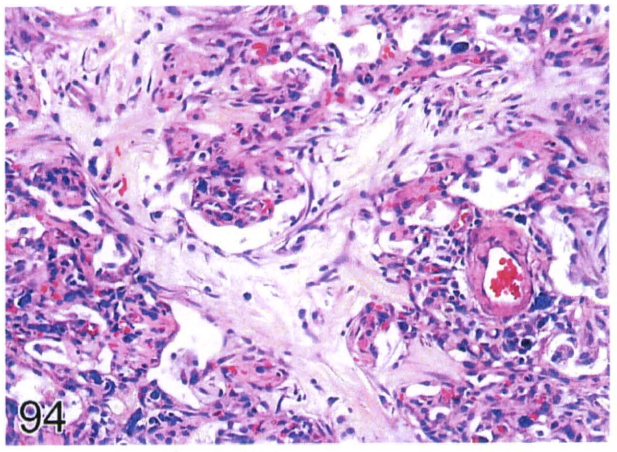

FIGURE 94.—Rat. Lung, well developed alveolar septal and interstitial fibrosis.

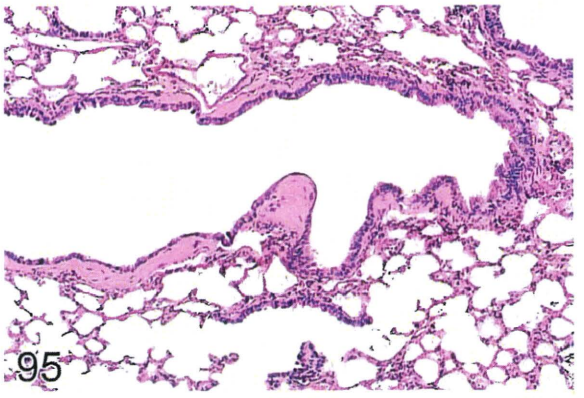

FIGURE 95.—Rat. Lung, fibrosis in wall of bronchiole.

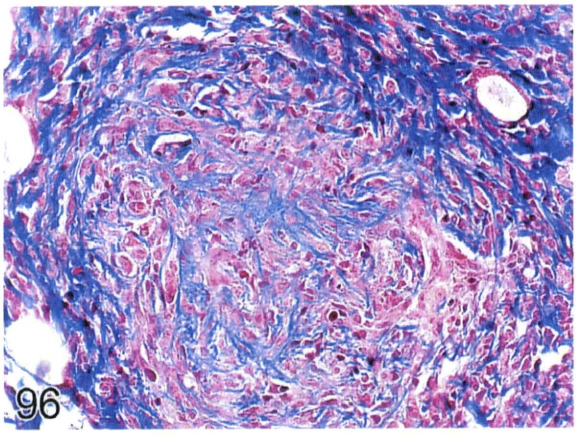

FIGURE 96.—Rat. Lung, pulmonary fibrosis, trichrome stain.

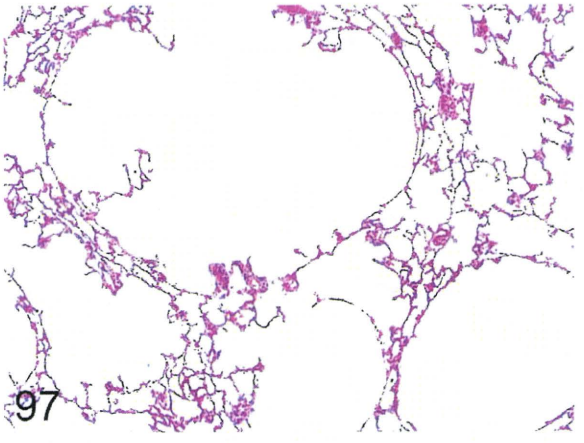

FIGURE 97.—Rat. Lung, artifactual pulmonary acinar ectasia due to overinflation with fixative.

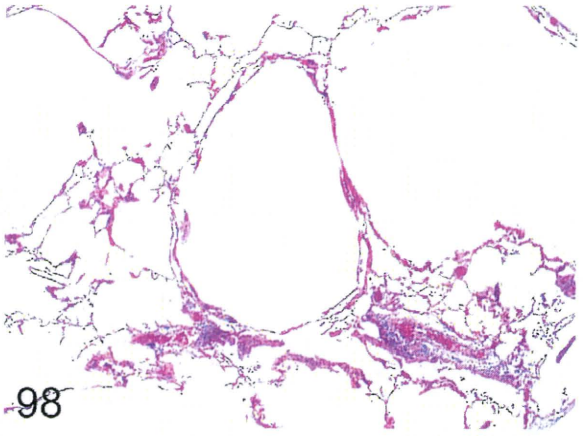

FIGURE 98.—Rat. Lung, alveolar emphysema induced by instillation of elastase.

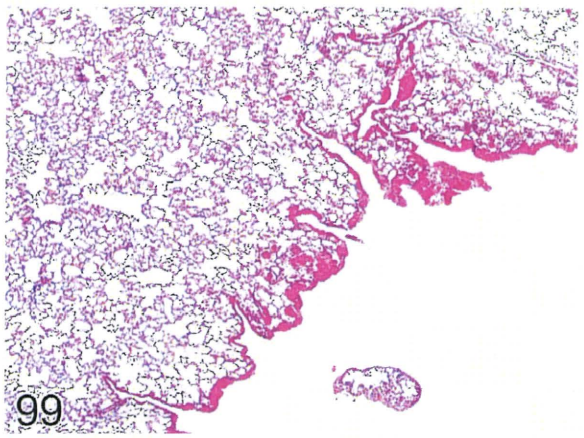

FIGURE 99.—Rat. Lung, alveolar hemorrhage from euthanasia with 100% carbon dioxide.

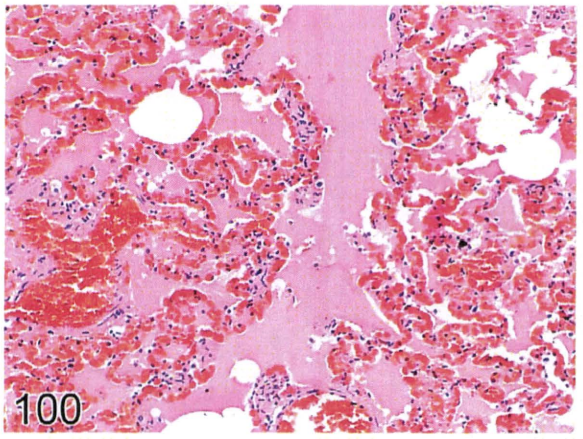

FIGURE 100.—Rat. Lung, severe congestion and edema.

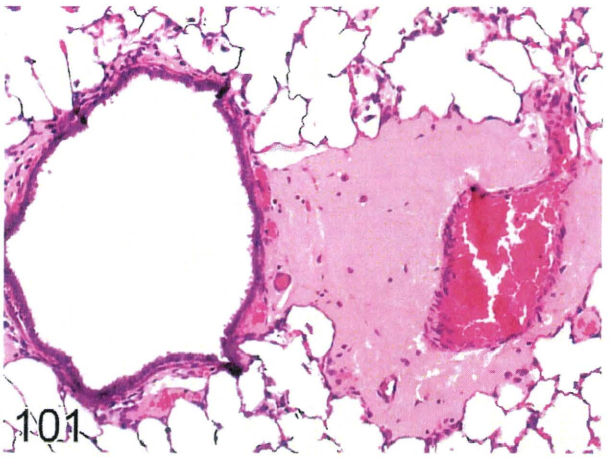

FIGURE 101.—Rat. Lung, perivascular and peribronchiolar edema.

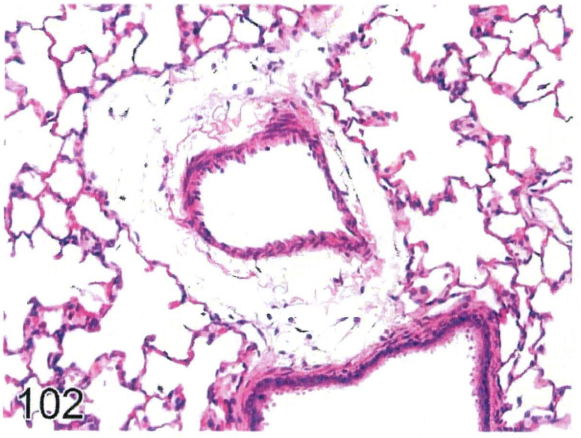

FIGURE 102.—Rat. Lung, artifactual increased perivascular space due to overinflation.

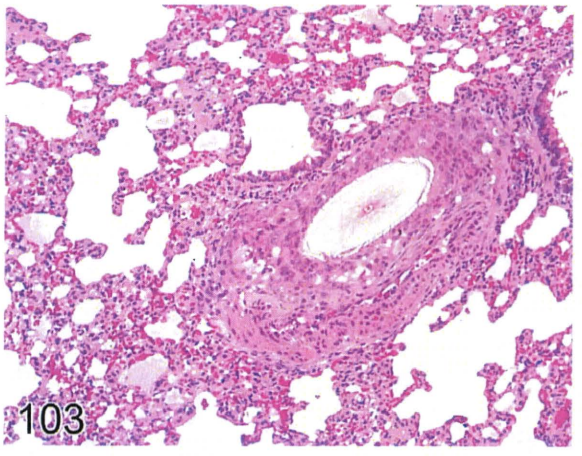

FIGURE 103.—Rat. Lung, foreign body embolus in pulmonary artery, polarized light.

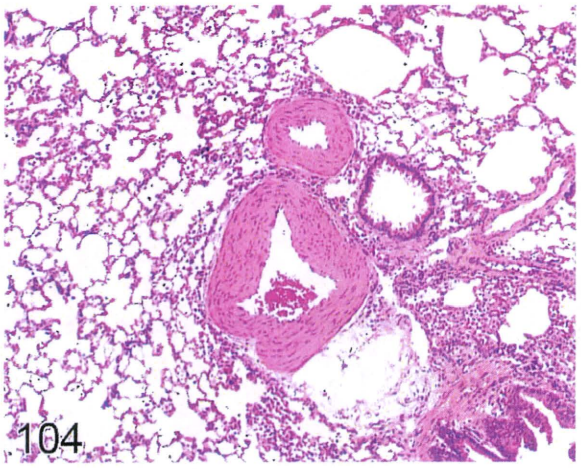

FIGURE 104.—Rat. Lung, medial hypertrophy of pulmonary artery.

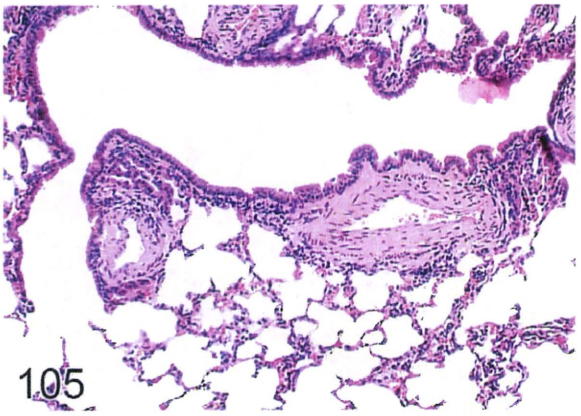

FIGURE 105.—Mouse. Lung, medial hypertrophy of pulmonary artery adjacent to bronchiole.

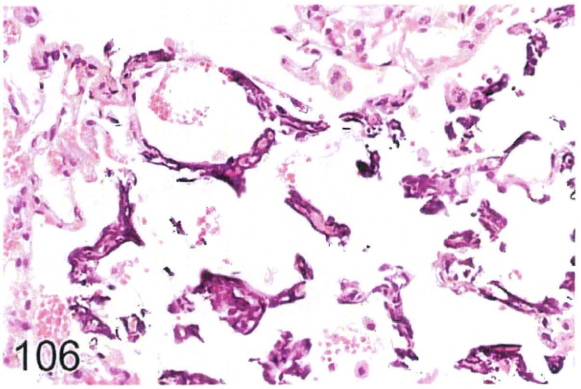

FIGURE 106.—Rat. Lung, mineralization of alveoli and pulmonary vessel.

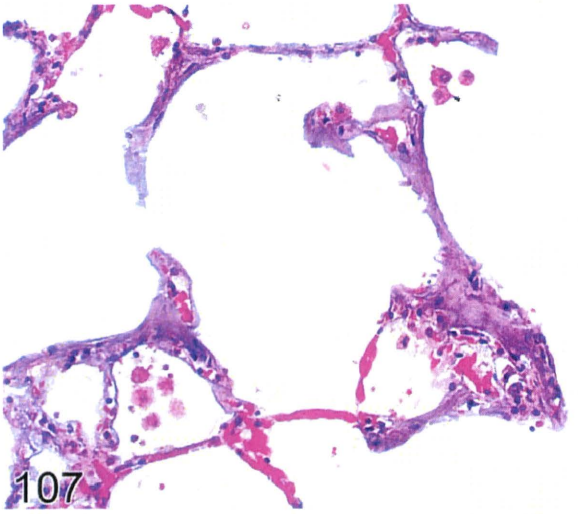

FIGURE 107.—Rat. Lung, severe mineralization of alveolar septa.

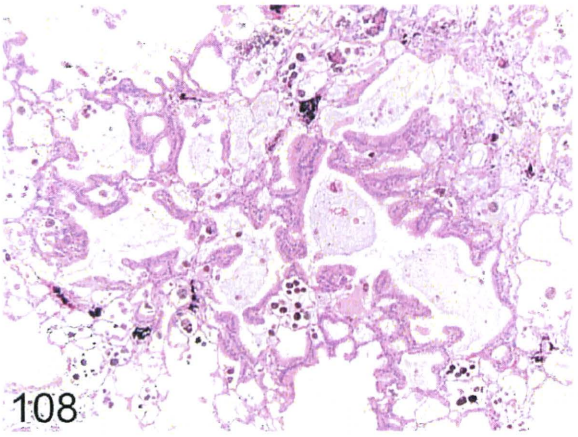

FIGURE 108.—Rat. Lung, bronchioloalveolar hyperplasia.

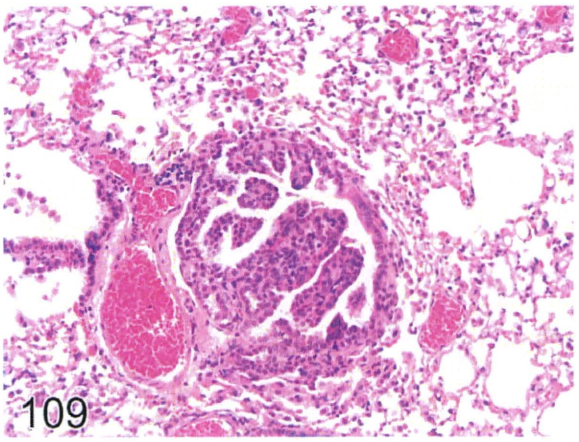

FIGURE 109.—Mouse. Lung, hyperplasia, bronchioalveolar in terminal bronchiole.

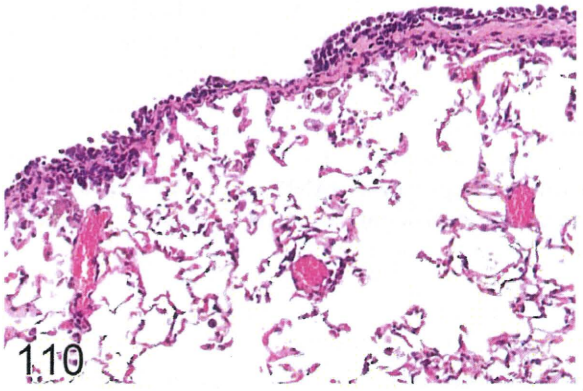

FIGURE 110.—Rat. Lung, mesothelial hyperplasia, visceral pleura.

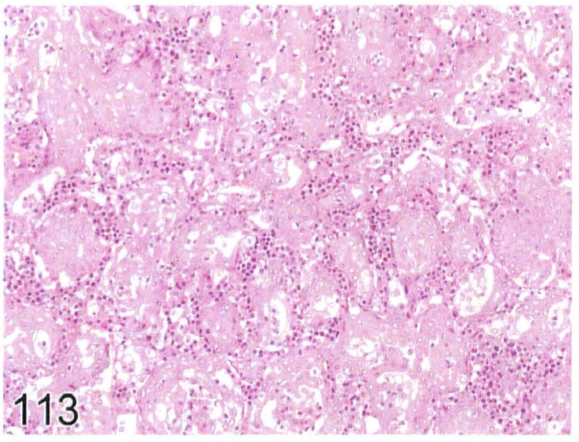

FIGURE 113.—Rat. Lung, epithelioma, nonkeratinizing.

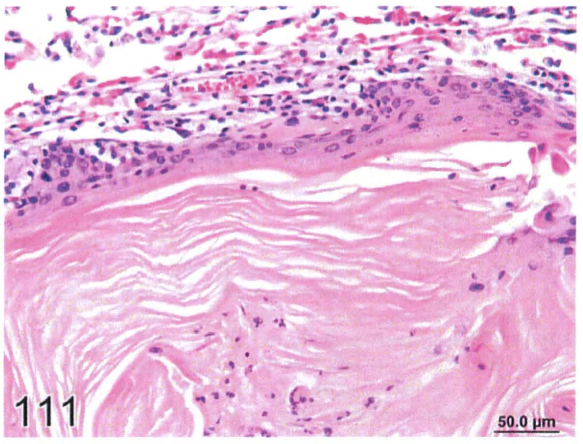

FIGURE 111.—Rat. Lung, pulmonary keratinizing cyst.

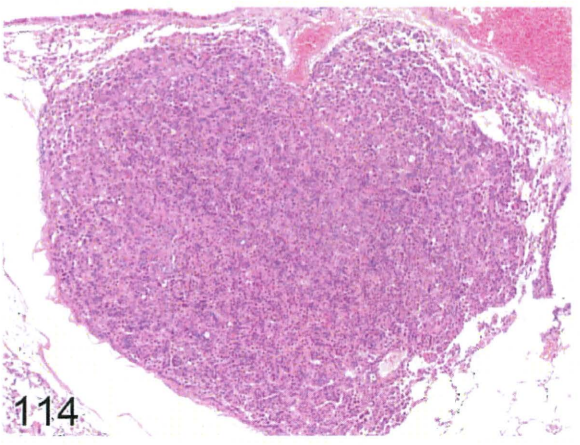

FIGURE 114.—Mouse. Lung, adenoma, bronchioloalveolar.

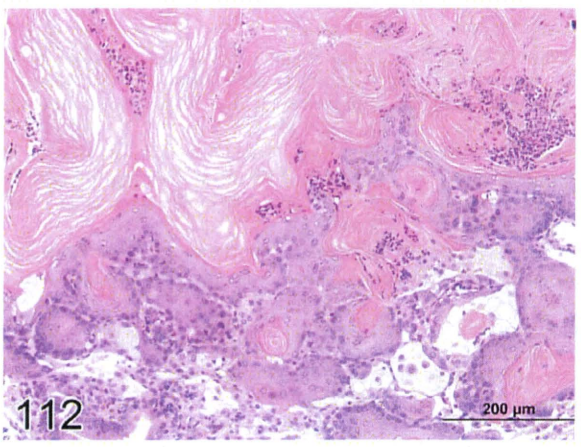

FIGURE 112.—Rat. Lung, cystic keratinizing epithelioma.

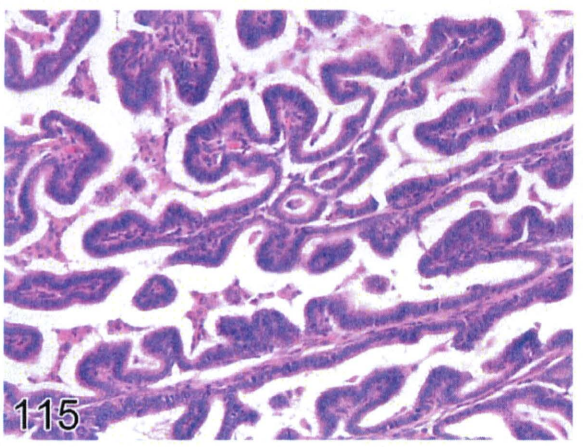

FIGURE 115.—Rat. Lung, carcinoma, bronchioloalveolar.

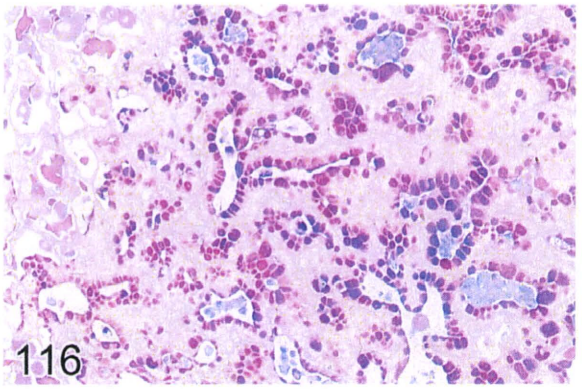

FIGURE 116.—Mouse. Lung, carcinoma, acinar.

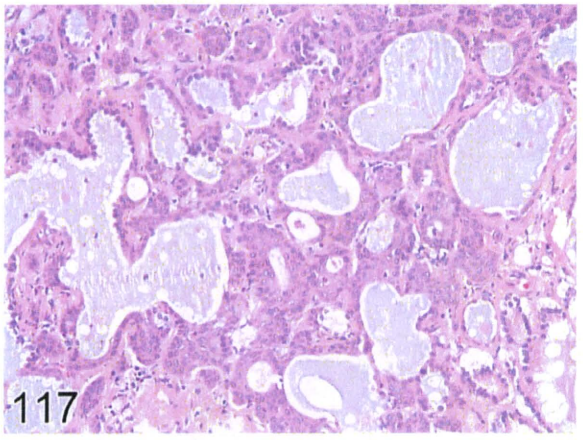

FIGURE 117.—Rat. Lung, carcinoma, adenosquamous.

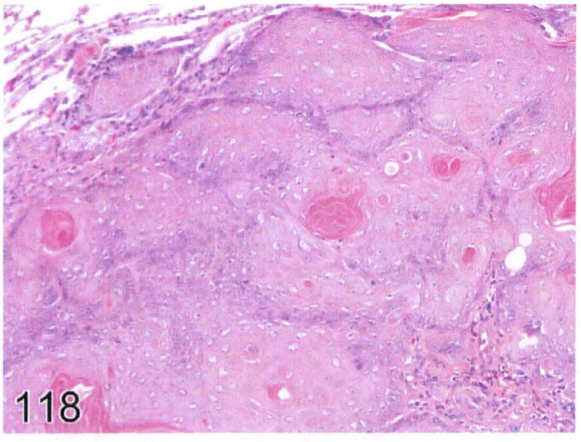

FIGURE 118.—Rat. Lung, carcinoma, squamous cell.

ACKNOWLEDGMENTS

The authors wish to express their appreciation for the excellent advice and assistance of Drs. Rodney Miller, Rani Sellers, Melvin Hamlin, Jerry Ward; the late Dr. Donald Dungworth; Beth Mahler; the staffs of the Cellular and Molecular Pathology Branch at the National Toxicology Program/National Institute of Environmental Health Sciences and the Fraunhofer Institute of Toxicology and Experimental Medicine in Hannover; the members of the ESTP, STP, JSTP, and BSTP who are participating in the INHAND project; and pathologists and other professional scientists worldwide whose work contributed to this document.

REFERENCES

Adams, D. R., Jones, A. M., Plopper, C. G., Serabjit-Singh, C. J., and Philpot, R. M. (1991). Distribution of cytochrome P-450 monoxygenase enzymes in the nasal mucosa of hamster and rat. *Am J Anat* **190**, 291–98.

Adriaensen, D., Scheuermann, D. W., Gajda, M., Brouns, I., and Timmermans, J. P. (2001). Functional implications of extensive new data on the innervation of pulmonary neuroepithelial bodies. *Ital J Anat Embryol* **106**, 395–403.

Baker, D. G. (1998). Natural pathogens of laboratory mice, rats, and rabbits and their effects on research. *Clin Microbiol Rev* **11**, 231–66.

Barrow, C. S., Buckley, L. A., James, R. A., Steinhagen, W. H., and Chang, J. F. (1986). Sensory irritation: Studies on correlation to pathology, structure-activity, tolerance development, and prediction of species differences to nasal injury. In Toxicology of the Nasal Passages (C. S. Barrow, ed.), pp. 101–22, Hemisphere Publishing Co., Washington, DC.

Beer, D. G., and Malkinson, A. M. (1985). Genetic influence on type 2 or Clara cell origin of pulmonary adenomas in urethan-treated mice. *J Natl Cancer Inst* **75**, 963–69.

Belinsky, S. A., Devereux, T. R., Foley, J. F., Maronpot, R. R., and Anderson, M. W. (1992). Role of the alveolar type II cell in the development and progression of pulmonary tumors induced by 4-(methylnitrosamino)-1-(3-pyridyl)-1-butanone in the A/J mouse. *Cancer Res* **52**, 3164–73.

Belinsky, S. A., Devereux, T. R., White, C. M., Foley, J. F., Maronpot, R. R., and Anderson, M. W. (1991). Role of Clara cells and type II cells in the development of pulmonary tumors in rats and mice following exposure to a tobacco-specific nitrosamine. *Exp Lung Res* **17**, 263–78.

Belinsky, S. A., Walker, V. E., Maronpot, R. R., Swenberg, J. A., and Anderson, M. W. (1987). Molecular dosimetry of DNA adduct formation and cell toxicity in rat nasal mucosa following exposure to the tobacco specific nitrosamine 4-(N-methyl-N-nitrosamino)-1-(3-pyridyl)-1-butanone and their relationship to induction of neoplasia. *Cancer Res* **47**, 6058–65.

Bermudez, E., Gross, E. A., Chen, Z., and Morgan, K. T. (1992). Isolation and characterization of cell lines from formaldehyde-induced rat nasal squamous cell carcinomas. *Toxicologist* **12**, 379.

Bermudez, E., Mangum, J. B., Asgharian, B., Wong, B. A., Reverdy, E. E., Janszen, D. B., Hext, P. M., Warheit, D. B., and Everitt, J. I. (2002). Long-term pulmonary responses of three laboratory rodent species to subchronic inhalation of pigmentary titanium dioxide particles. *Toxicol Sci* **70**, 86–97.

Bermudez, E., Mangum, J. B., Wong, B. A., Asgharian, B., Hext, P. M., Warheit, D. B., and Everitt, J. I. (2004). Pulmonary responses of mice, rats, and hamsters to subchronic inhalation of ultrafine titanium dioxide particles. *Toxicol Sci* **77**, 347–57.

Bogdanffy, M. S. (1990). Biotransformation enzymes in the rodent nasal mucosa: The value of a histochemical approach. *Environ Health Perspect* **85**, 177–86.

Bond, J. A. (1986). Bioactivation and biotransformation of xenobiotics in rat nasal tissue. In Toxicology of the Nasal Passages (C. S. Barrow, ed.), pp. 249–61, Hemisphere Publishing Co, Washington.

Boorman, G. A. (1985a). Bronchiolar/alveolar adenoma, lung, rat. In Monographs on Pathology of Laboratory Animals. Respiratory System (T. C. Jones, U. Mohr, and R. D. Hunt, eds,), pp. 99–101, Springer, Berlin, Heidelberg, New York, Tokyo.

Boorman, G. A. (1985b). Bronchiolar/alveolar carcinoma, lung, rat. In Monographs on Pathology of Laboratory Animals. Respiratory System (T. C. Jones, U. Mohr, and R. D. Hunt, eds,), pp 112–16, Springer, Berlin, Heidelberg, New York, Tokyo.

Boorman, G. A. (1985c). Squamous cell carcinoma, lung, rat. In Monographs on Pathology of Laboratory Animals. Respiratory System (T. C. Jones, U. Mohr, and R. D. Hunt, eds,), pp. 124–27, Springer, Berlin, Heidelberg, New York, Tokyo.

Boorman, G. A., Brockmann, M., Carlton, W. W., Davis, J. M., Dungworth, D. L., Hahn, F. F., Mohr, U., Reichhelm, H. B., Turosov, V. S., and Wagner, B. M. (1996). Classification of cystic keratinizing squamous lesions of the rat lung: Report of a workshop. *Toxicol Pathol* **24**, 564–72.

Boorman, G. A., and Eustis, S. L. (1990). Lung. In Pathology of the Fischer Rat. Reference and Atlas (G. A. Boorman, S. L. Eustis, M. R. Elwell, C. A. Montgomery Jr, and W. F. MacKenzie, eds.), pp. 339–67, Academic Press, San Diego, New York, London.

Boorman, G. A., Morgan, K. T., and Uraih, L. C. (1990) Nose, larynx, and trachea. In Pathology of the Fischer Rat. Reference and Atlas (G. A. Boorman, S. L. Eustis, M. R. Elwell, C. A. Montgomery Jr, and W. F. MacKenzie, eds.), pp. 315–37, Academic Press, San Diego, New York, London.

Boros, D. L. (1978). Granulomatous inflammations. *Prog Allergy* **24**, 183–267.

Brandsma, A. E., ten Have-Opbroek, A. A., Vulto, I. M., Molenaar, J. C., and Tibboel, D. (1994). Alveolar epithelial composition and architecture of the late fetal pulmonary acinus: An immunocytochemical and morphometric study in a rat model of pulmonary hypoplasia and congenital diaphragmatic hernia. *Exp Lung Res* **20**, 491–515.

Branstetter, D. G., and Moseley, P. P. (1991). Effect of lung development on the histological pattern of lung tumors induced by ethylnitrosourea in the C3HeB/FeJ mouse. *Exp Lung Res* **17**, 169–79.

Breeze, R. G., and Wheeldon, E. B. (1977). The cells of the pulmonary airways. *Am Rev Respir Dis* **116**, 705–77.

Brix, A. E., Jokinen, M. P., Walker, N. J., Sells, D. M., and Nyska, A. (2004). Characterization of bronchiolar metaplasia of the alveolar epithelium in female Sprague-Dawley rats exposed to 3,3′,4,4′,5-pentachlorobiphenyl (PCB126). *Toxicol Pathol* **32**, 333–37.

Brix, A. E., Nyska, A., Haseman, J. K., Sells, D. M., Jokinen, M. P., and Walker, N. J. (2005). Incidences of selected lesions in control female Harlan Sprague-Dawley rats from two-year studies performed by the National Toxicology Program. *Toxicol Pathol* **33**, 477–83.

Brown, H. R. (1990). Neoplastic and potentially preneoplastic changes in the upper respiratory tract of rats and mice. *Environ Health Perspect* **85**, 291–304.

Brown, H. R., Monticello, T. M., Maronpot, R. R., Randall, H. W., Hotchkiss, J. R., and Morgan, K. T. (1991) Proliferative and neoplastic lesions in the rodent nasal cavity. *Toxicol Pathol* **19**, 358–72.

Bucher, J. R., Elwell, M. R., Thompson, M. B., Chou, B. J., Renne, R., and Ragan, H. A. (1990). Inhalation toxicity studies of cobalt sulfate in F344/N rats and B6C3F1 mice. *Fundam Appl Toxicol* **15**, 357–72.

Buchweitz, J. P., Harkema, J. R., and Kaminski, N. E. (2007). Time-dependent airway epithelial and inflammatory cell responses induced by influenza virus A/PR/8/34 in C57BL/6 mice. *Toxicol Pathol* **35**, 424–35.

Buckley, L. A., Jiang, X. Z., James, R. A., Morgan, K. T., and Barrow, C. S. (1984). Respiratory tract lesions induced by sensory irritants at the RD50 concentration. *Toxicol Appl Pharmacol* **74**, 417–29.

Buckley, L. A., Morgan, K. T., Swenberg, J. A., James, R. A., Hamm, T. E., and Barrow, C. S. (1985). The toxicity of dimethylamine in F-344 rats and B6C3F1 mice following a 1-year inhalation exposure. *Fundam Appl Toxicol* **5**, 341–52.

Burton, F. G., Clark, M. L., Miller, R. A., and Schirmer, R. E. (1982) Generation and characterization of red phosphorus smoke aerosols for inhalation exposure of laboratory animals. *Am Ind Hyg Assoc J* **43**, 767–72.

Busch, R. H., Lauhala, K. E., Loscutoff, S. M., and McDonald, K. E. (1984). Experimental pulmonary emphysema induced in the rat by intratracheally administered elastase: Morphogenesis. *Environ Res* **33**, 497–513.

Castleman, W. L. (1992). Effects of infectious agents and other factors on the lungs. In Pathobiology of the Aging Rat, Vol. 1 (U. Mohr, D. L. Dungworth, and C. C. Capen, eds), pp. 181–91, ILSI Press, Washington, DC.

Chandra, M., Riley, M. G. I., and Johnson, D. E. (1991). Clear-cell carcinoma in the trachea of a rat. *Lab Anim Sci* **41**, 262–64.

Chen, H. C., Pan, I. Z., Liang, C. T., and Hong, C. C. (1995). Nasal adenocarcinoma with myoepithelial component in a CD-1 mouse. *Vet Pathol* **32**, 710–13.

Dahl, A. R. (1986). Possible consequences of cytochrome P-450-dependent monooxygenases in nasal tissues. In Toxicology of the Nasal Passages (C. S. Barrow, ed), pp. 263–73, Hemisphere Publishing Co, Washington, DC.

Dickhaus, S., Reznik, G., Green, U., and Ketkar, M. (1977). The carcinogenic effect of beta-oxidized dipropylnitrosamine in mice. I. Dipropylnitrosamine and methyl-propylnitrosamine. *Z Krebsforsch* **90**, 253–58.

Dickhaus, S., Reznik, G., Green, U., and Ketkar, M. (1978). The carcinogenic effect of beta oxydized dipropylnitrosamine in mice. II. 2-hydroxypropyl-n-propylnitrosamine and 2-oxo-propyl-n-propylnitrosamine. *Z Krebsforsch* **91**, 189–93.

Dixon, D., Horton, J., Haseman, J. K., Talley, F., Greenwell, A., Nettesheim, P., Hook, G. E., and Maronpot, R. R. (1991). Histomorphology and ultrastructure of spontaneous pulmonary neoplasms in strain A mice. *Exp Lung Res* **17**, 131–55.

Dixon, D., and Maronpot, R. R. (1991). Histomorphologic features of spontaneous and chemically-induced pulmonary neoplasms in B6C3F1 mice and Fischer 344 rats. *Toxicol Pathol* **19**, 540–56.

Dorman, D. C., Brenneman, K. A., McElveen, A. M., Lynch, S. E., Roberts, K. C., and Wong, B. A. (2002). Olfactory transport: A direct route of delivery of inhaled manganese phosphate to the rat brain. *J Toxicol Environ Health A* **65**, 1493–511.

Driscoll, K. (1995). Role of cytokines in pulmonary inflammation and fibrosis. In Concepts in Inhalation Toxicology (R. O. McClellan and R. F. Henderson, eds.), pp. 471–504, Taylor and Francis, Washington, DC.

Dungworth, D. L., Ernst, H., Nolte, T., and Mohr, U. (1992). Nonneoplastic lesions in the lungs. In Pathobiology of the Aging Rat, Vol. 1 (U. Mohr, C. C. Capen, and D. L. Dungworth, eds.), pp. 143–60, ILSI Press, Washington.

Dungworth, D. L., Hahn, F. F., Hayashi, Y., Keenan, K., Mohr, U., Rittinghausen, S., and Schwartz, L. (1992). 1. Respiratory system. In International classification of rodent tumours. Part I: The rat (U. Mohr, C. C. Capen, D. L. Dungworth, R. A. Griesemer, N. Ito, and V. S. Turusov, eds.), pp, 1–57, IARC Scientific Publications No. 122, Lyon, France.

Dungworth, D. L., Hahn, F. F., and Nikula, K. J. (1995). Noncarcinogenic responses of the respiratory tract to inhaled toxicants. In Concepts in Inhalation Toxicology (R. O. McClellan and R. F. Henderson, eds.), pp. 533–76, Taylor and Francis, Washington, DC.

Dungworth, D. L., Rittinghausen, S., Schwartz, L., Harkema, J. R., Hayashi, Y., Kittel, B., Lewis, D., Miller, R. A., Mohr, U., Morgan, K. T., Rehm, S., and Slayter, M. V. (2001). Respiratory system and mesothelium. In International Classification of Rodent Tumors: The mouse (U. Mohr, ed.), pp. 93–94, Springer, Berlin, Heidelberg, New York.

Elder, A., Gelein, R., Finkelstein, J. N., Driscoll, K. E., Harkema, J., and Oberdorster, G. (2005). Effects of subchronically inhaled carbon black in three species. I. *Toxicol Sci* **88**, 614–29.

Elizegi, E., Pino, I., Vicent, S., Blanco, D., Saffiotti, U., and Montuenga, L. M. (2001). Hyperplasia of alveolar neuroendocrine cells in rat lung carcinogenesis by silica with selective expression of proadrenomedullin-derived peptides and amidating enzymes. *Lab Invest* **81**, 1627–38.

Elkon, D. (1983). Olfactory esthesioneuroblastoma. In Nasal Tumours in Animals and Man. Vol II: Tumour pathology (G. Reznik and S. F. Stinson, eds.), pp. 129–47, CRC Press, Boca Raton, FL.

Ernst, H., Dungworth, D. L., Kamino, K., Rittinghausen, S., and Mohr, U. (1996). Nonneoplastic lesions in the lungs. In Pathobiology of the Aging Mouse, Vol. 1 (U. Mohr, D. L. Dungworth, C. C. Capen, W. W. Carlton, J. P. Sundberg, and J. M. Ward, eds.), pp. 281–300, ILSI Press, Washington, DC.

Everitt, J. I., Bermudez, E., Mangum, J. B., Wong, B., Moss, O. M., Janszen, D., and Rutten, A. A. (1994). Pleural lesions in Syrian Golden hamsters